The Development of Snow Multi-Bands in High-Resolution Idealized Baroclinic Wave Simulations

Nicholas Leonardo and Brian A. Colle

Acknowledgment: Phillip Yeh (grad student)

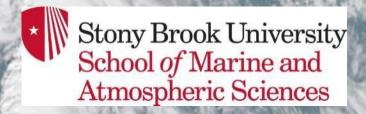
¹School of Marine and Atmospheric Sciences, Stony Brook Univ.

27 February 2024





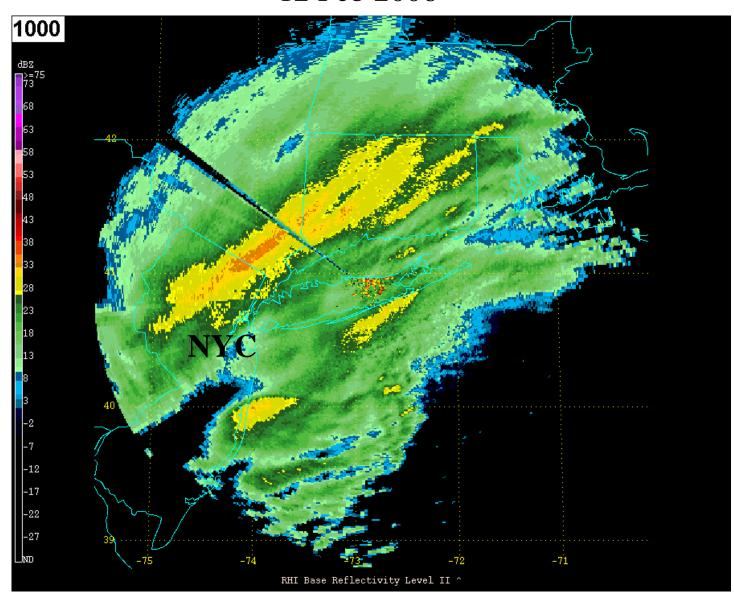




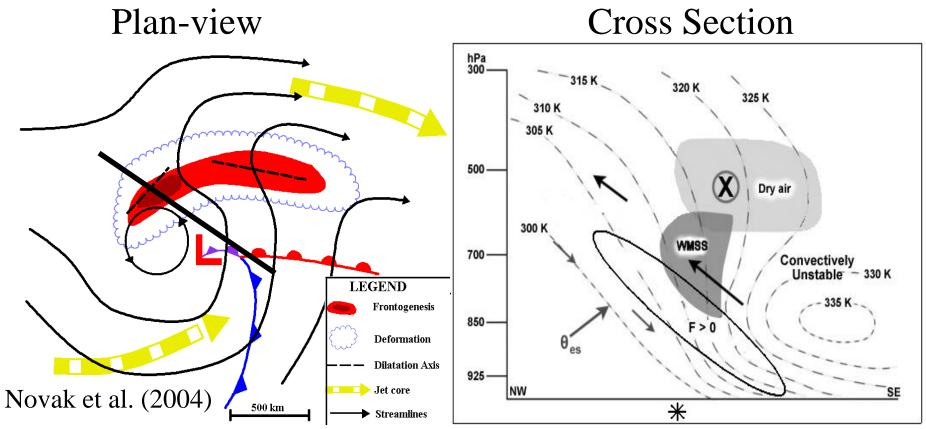
The Challenge of Snowbands in Winter Storms

12 Feb 2006

- Bands make
 Quantitative
 Precipitation Forecasts
 (QPF) difficult
 - Localized heavy precipitation
 - Extreme gradients
 - Evolution



Conceptual Model for "Primary" Band

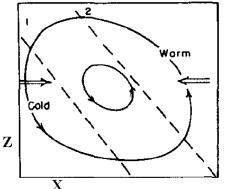


Novak et al. (2006) (adapted from Moore et al. 2005)

Frontogenesis in the presence of weak moist symmetric stability and sufficient moisture

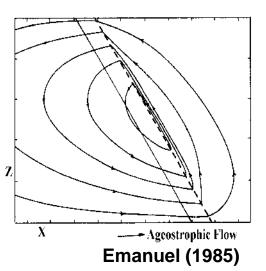
Band Ingredients and Transition to Multi-Bands

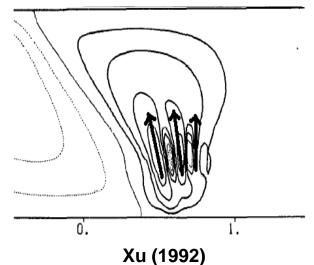
Lift – Frontogenesis

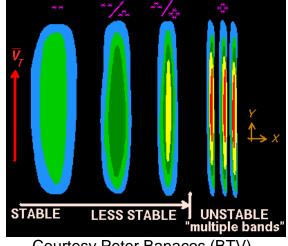


Sanders and Bosart (1985)

Instability— weak moist (conditional or potential) symmetric stability







Courtesy Peter Banacos (BTV)

Moisture

Many Smaller-Bands Have Weak or No Frontogenesis

700-800 hPa Frontogenesis vs Instability (neg MPV*)

Ganetis et al. (2018) (c) (d) (e) No Bands Largest 1/3 bands Smallest 2/3 bands 700 hPa Frontogenesis (K 100 km^{-1} h^{-1}) 700 hPa Frontogenesis 700 hPa Frontogenesis K 100 km 750-650 hPa Average MPV* 750-650 hPa Average MPV* 750-650 hPa Average MPV* Distribution of 800-700 hPa Average Frontogenesis SINGLE 800-700 hPa Frontogenesis Many bands occur with limited mid-level frontogenesis - Ganetis et al. (2018) BOTH-MID SUBSET $(K 100 km^{-1} h)$ NONE 50 200 250 Profiles Sorted by Frontogenesis

Importance of Vertical Shear for Multi-bands?

NOVEMBER 2018

GANETIS ET AL.

TABLE 3. Environmental banding ingredients for each classification type.

| | 700-hPa frontogenesis $[K (100 \text{ km})^{-1} \text{ h}^{-1}]$ | 700-hPa MPV* (PVU) | 750–650-hPa dT/dP (×10 ⁻⁴ °C Pa ⁻¹) | 750–650-hPa $d\theta_e^*/dP$ (×10 ⁻⁴ K Pa ⁻¹) | 950–750-hPa wind speed difference $(m s^{-1})$ |
|---------------------|------------------------------------------------------------------|-----------------------|-----------------------------------------------------------------|-------------------------------------------------------------------------|------------------------------------------------|
| SINGLE | 0.90 | -0.77 | -4.98 | 4.84 | 3.71 |
| MULTI | 0.13 | -0.53 | -4.71 | 5.04 | 5.84 |
| BOTH-Large bands | 0.99 | -0.75 | -3.08 | 8.04 | 3.01 |
| BOTH-Midsized bands | 0.14 | -0.54 | -4.55 | 5.36 | 5.67 |
| NONE | 0.12 | -0.63 | -4.68 | 5.32 | 10.51 |

Ganetis et al. 2018

3685

- Multibands & BOTH-Midsized were found to exist in weak frontogenesis
 - Frontogenesis is theorized origin of primary/single snowbands
- Enhanced vertical wind shear (hereafter referred to as "shear") was observed to exist in environments with multibands & BOTH-Midsized

Other Possible Mechanisms? "Snowbands" with Elevated Cells and Fallout; Organization from Vertical Shear and Deformation?

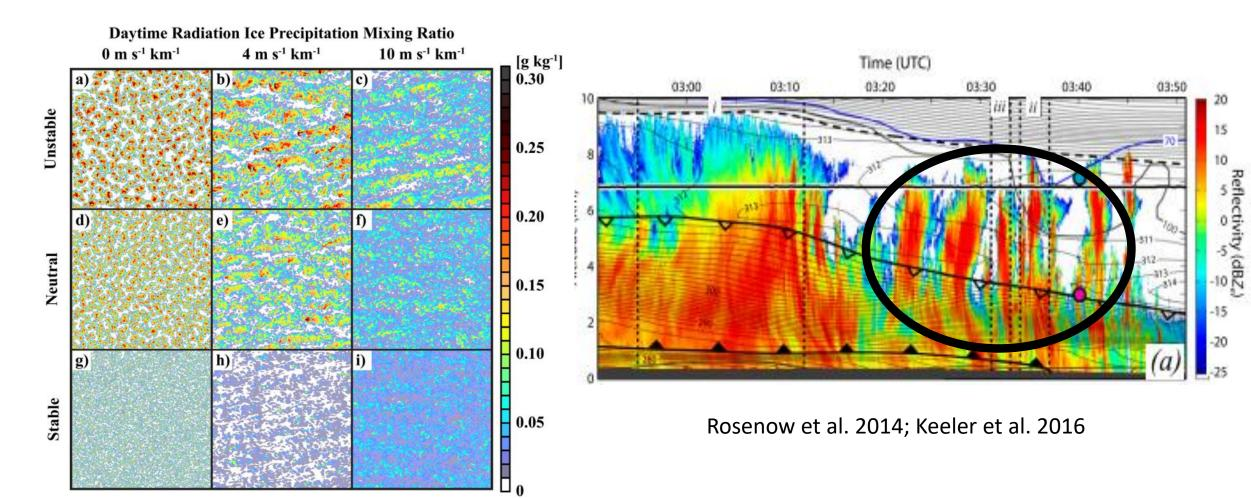


FIG. 13. As in Fig. 9, but for the daytime radiation simulations.

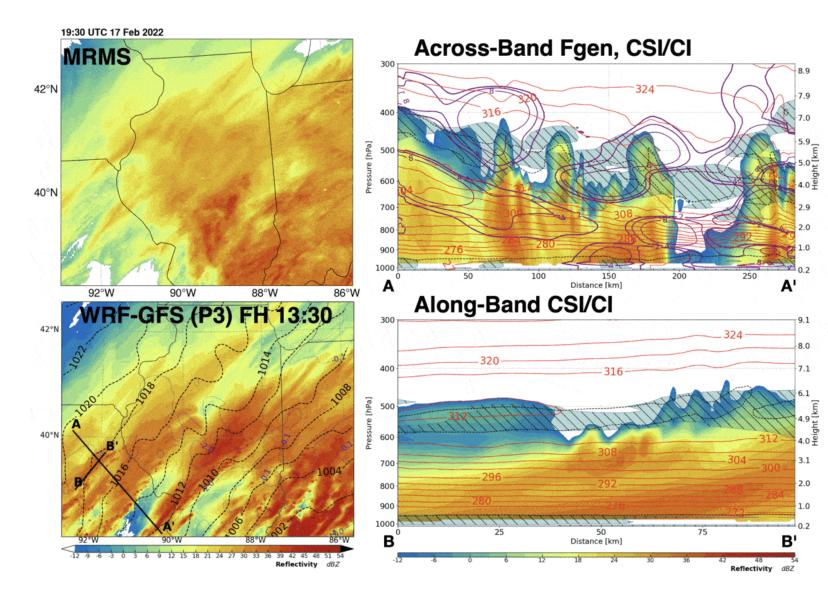
Keeler et al. 2017

17 Feb 2022

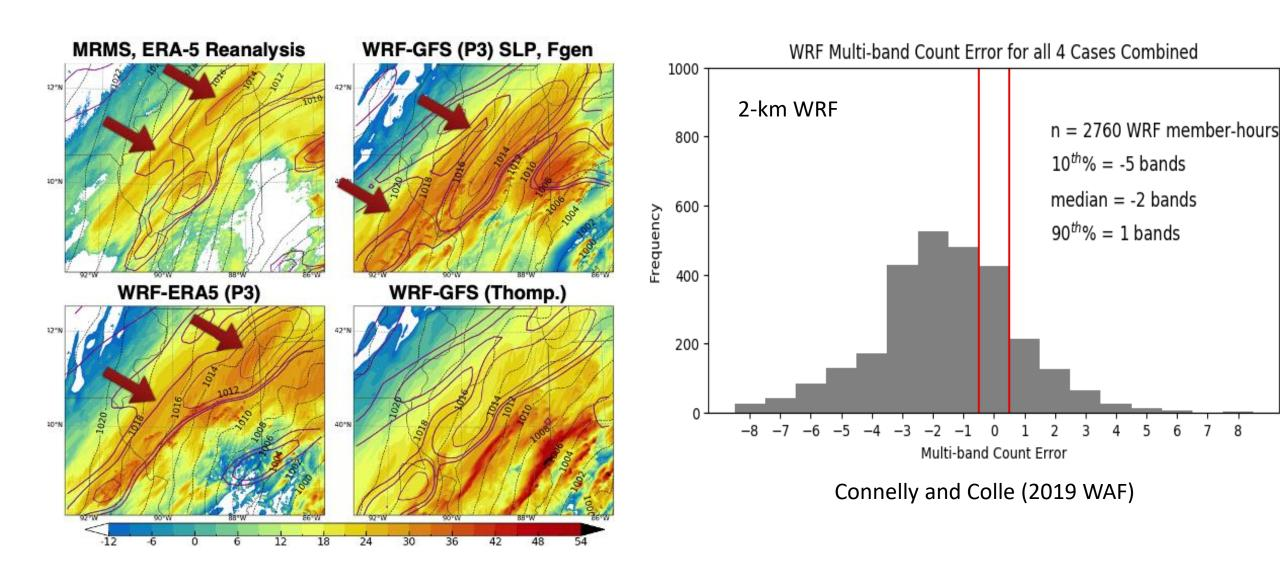
Band Evolution

- Precipitation structures become band-like over time
- Sloping region of frontogenesis (purple contours)
- Cloud-top instability
- 2-km WRF section: possible fallout from generating cells

IMPACTS Case: 1930~2330 UTC 17 Feb

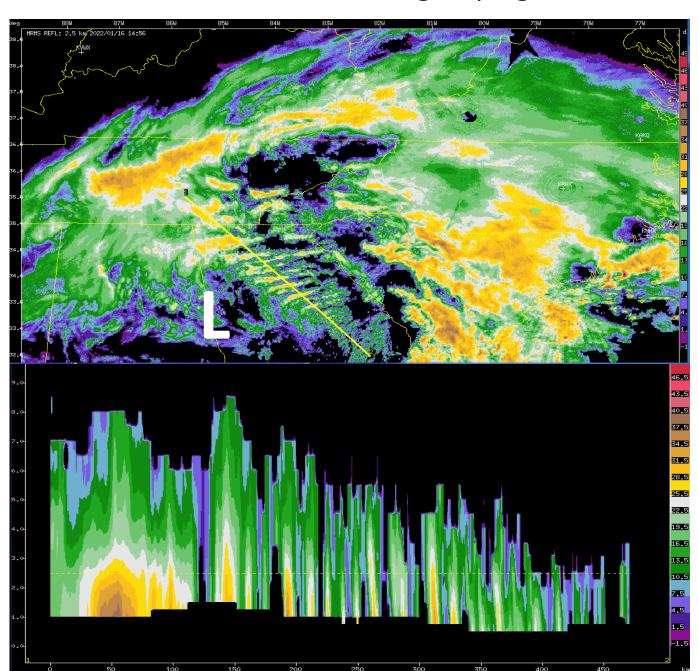


Predictability Challenges – Convective Resolving Models

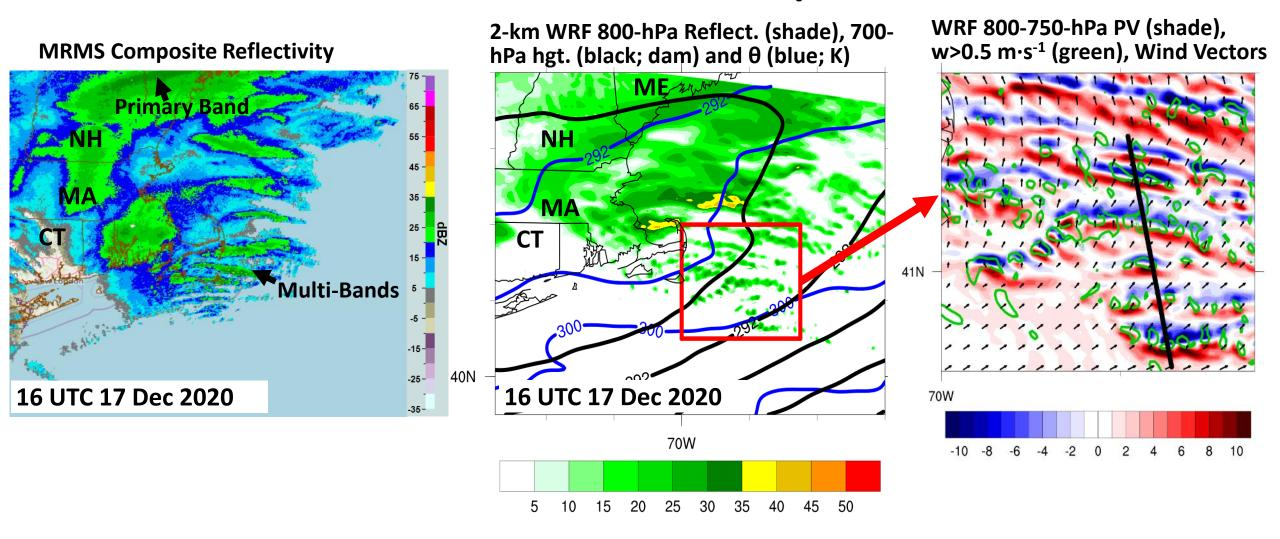


More Convective-Plume Multi-bands Along Sloping Baroclinic Zone

1500 UTC 16 Jan 2022



Multi-bands and PV Dipoles



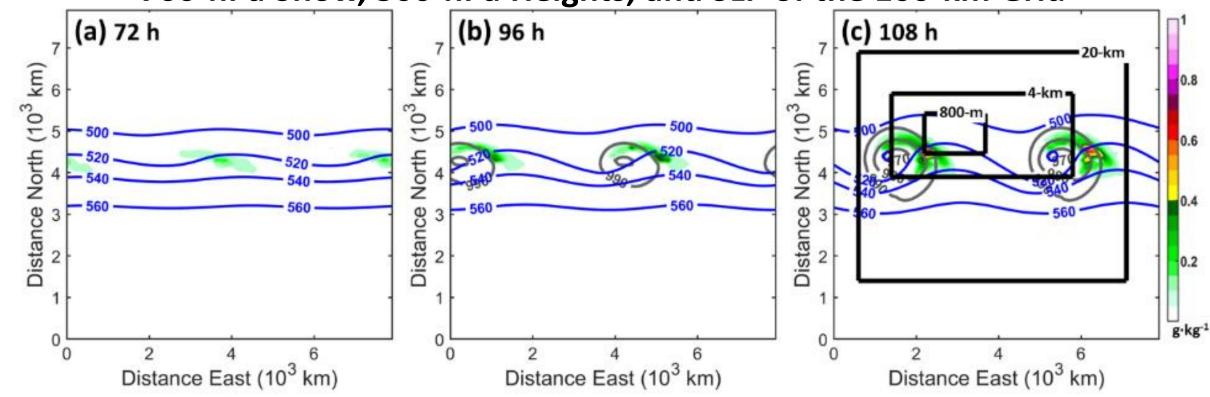
- Multi-bands in some cases are accompanied by PV dipoles
- Use idealized models to better isolate processes

Objectives

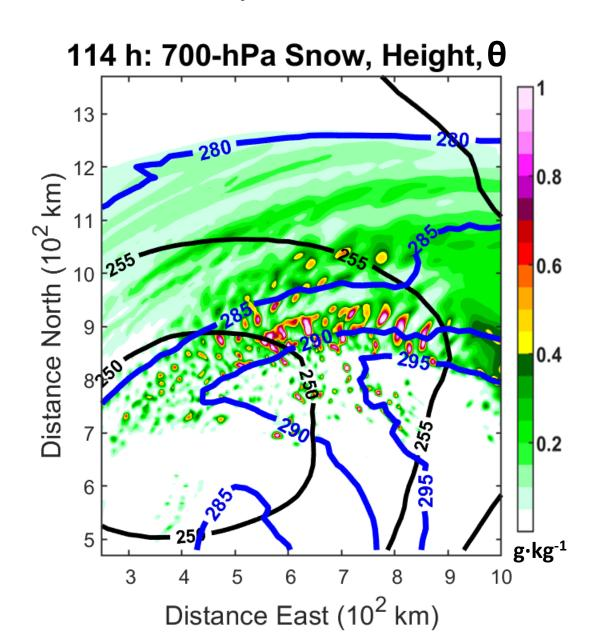
- Nested runs of an idealized baroclinic wave model are used to answer the following questions:
 - 1. How do the precipitation structures in the comma head evolve as the cyclone develops?
 - 2. How do changes in the ambient frontogenesis (forcing), vertical shear, and instability around the cyclone relate to changes in the precipitation structures.
 - 3. What mechanisms cause the bands to elongate and persist?
 - 4. How sensitive is the development of the multi-bands to small changes in the initial conditions?

Idealized Baroclinic Wave Model Setup

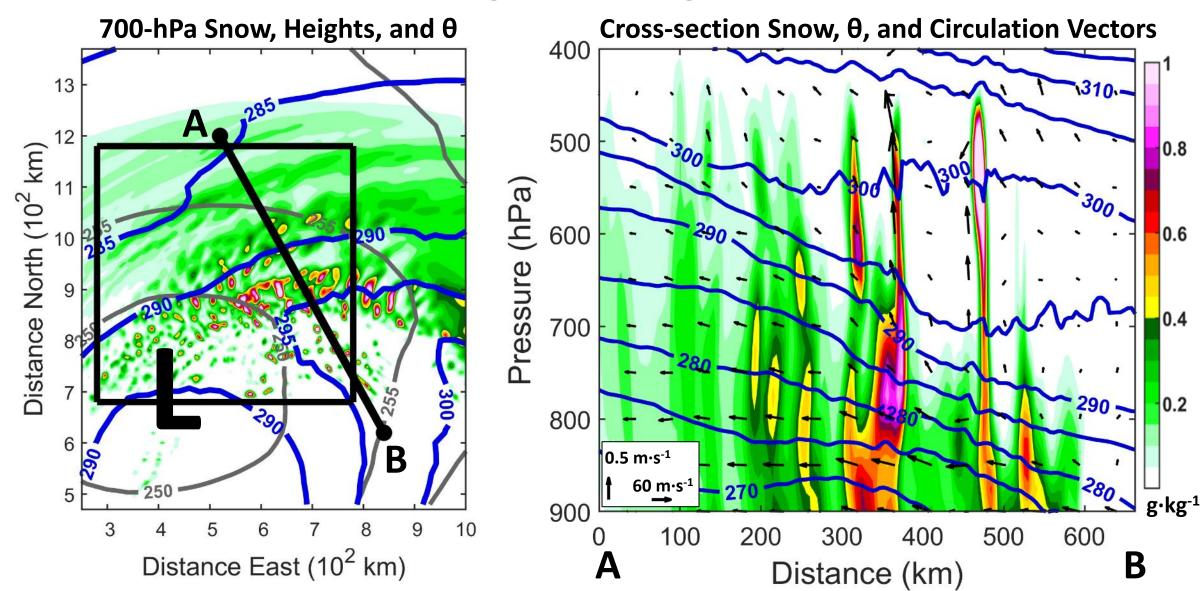
700-hPa Snow, 500-hPa Heights, and SLP of the 100-km Grid



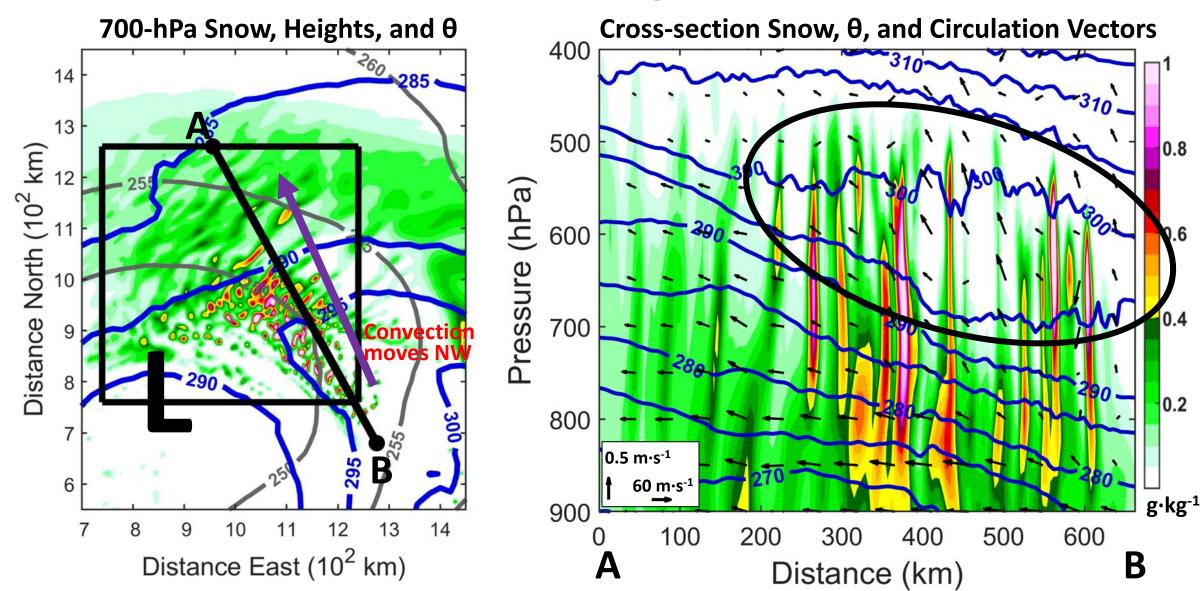
- Ran the baroclinic wave test case of WRF v3.4.1. Used physics consistent with Norris et al. 2014 and 2017: Thompson microphysics, YSU PBL, and Kain-Fritsch convection.
- 20-km and 4-km nests added at 108 h (panel c).
- 800-m added between 114 h and 132 h to capture the peak in band activity. There are similarities between the 4-km and 800-m, such that the 4-km will primarily be shown.



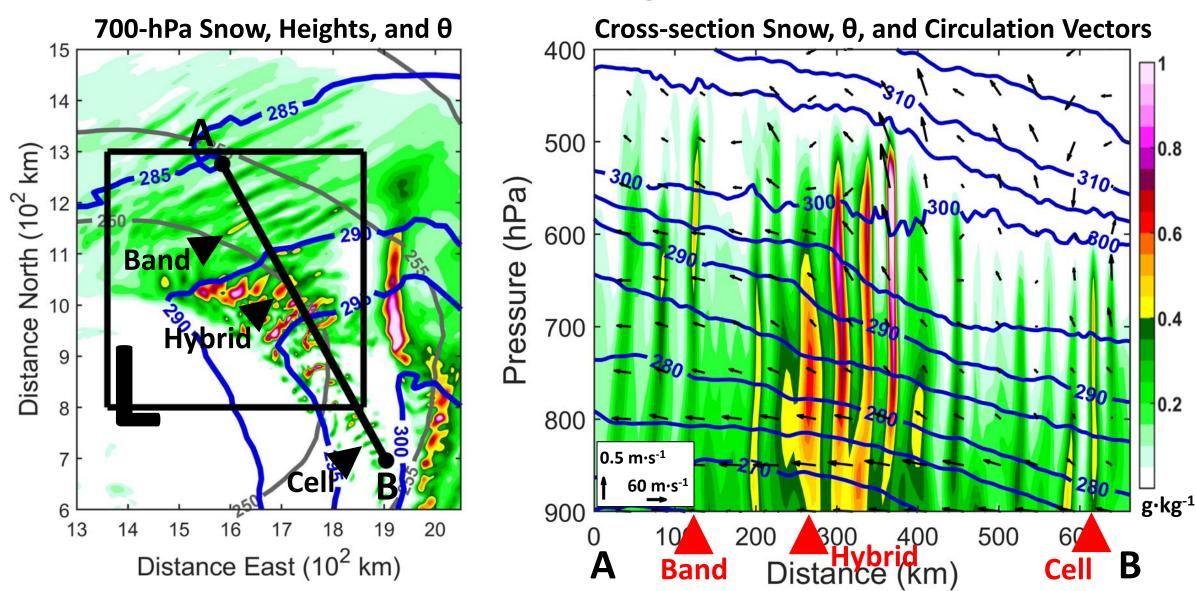
Pre-genesis Stage: 114 h



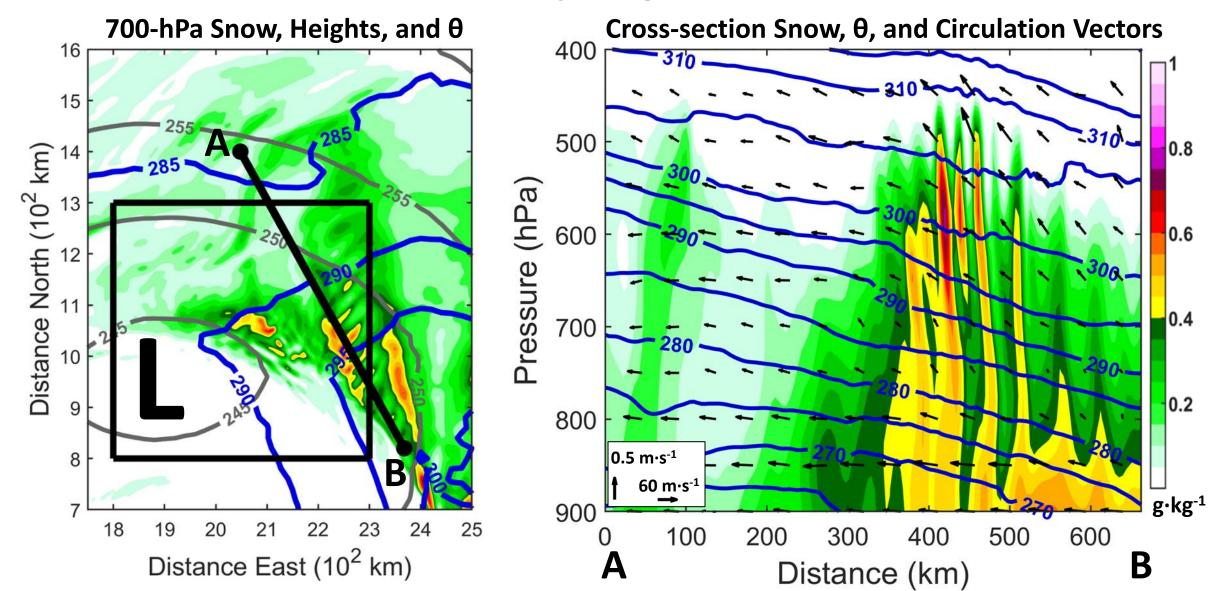
Genesis Stage: 120 h



Mature Stage: 129 h



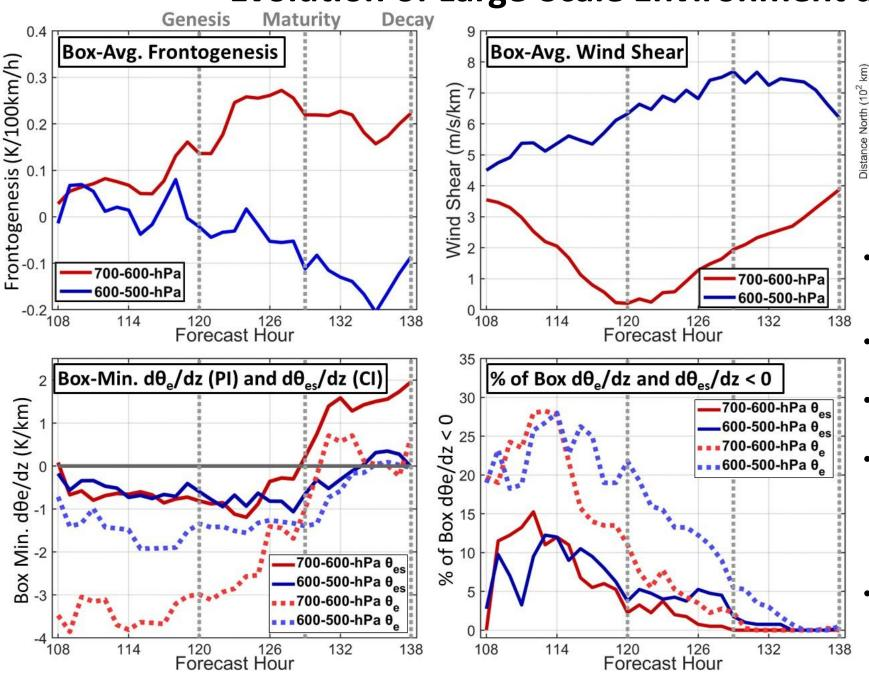
Decay Stage: 138 h

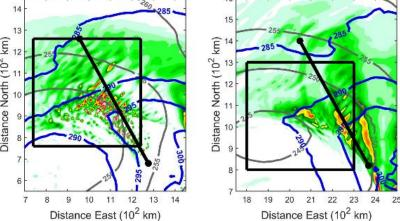


Evolution of Large-Scale Environment and Forcing

Leonardo and Colle (MWR in press 2024)

Evolution of Large-Scale Environment and Forcing



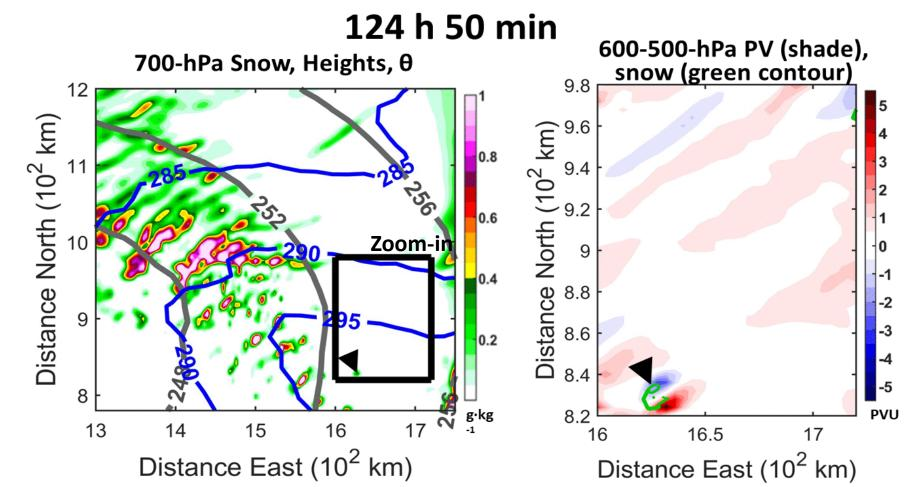


- Assess the forcing/instability in the 20-km grid. Took statistics within a box following the band activity.
- 700-600-mb fgen grows through genesis up to ~127 h.
- 600-500-mb SW (band-parallel) shear increases up to ~130 h.
- 600-500-hPa potential instability (PI) is largest 115-118 h, reaching 0 by 135-138 h during decay. Conditional instability (CI) is half of PI's amplitude/extent.
- PI/CI grow due to differential advection, from drier air aloft wrapping in from behind the system.

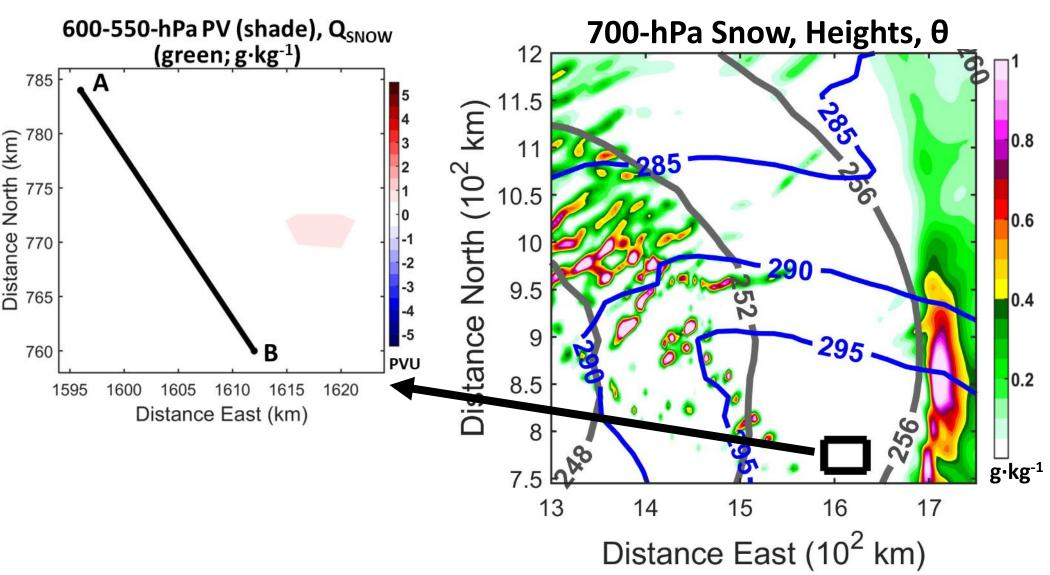
Objectives

- Nested runs of an idealized baroclinic wave model are used to answer the following questions:
 - 1. How do the precipitation structures in the comma head evolve as the cyclone develops?
 - 2. How do changes in the ambient frontogenesis (forcing), vertical shear, and instability around the cyclone relate to changes in the precipitation structures.
 - 3. What mechanisms cause the bands to elongate and persist?
 - 4. How sensitive is the development of the multi-bands to small changes in the initial conditions?

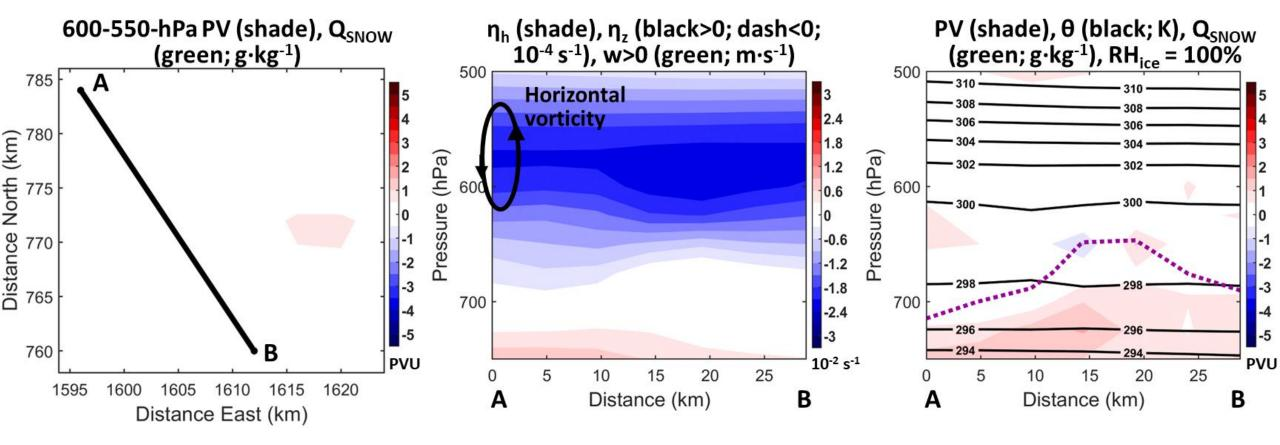
- Tracked a cell that later grows into a SW-NE band as it moves around the NE flank of the low.
- An upper-level potential vorticity (PV) dipole extends NE of the cell, along which new convection develops afterwards.
- PV dipoles have been associated with the organization of warm convection (e.g., Chagnon and Gray 2009; Moon and Nolan 2015; Hitchman and Rowe 2019).



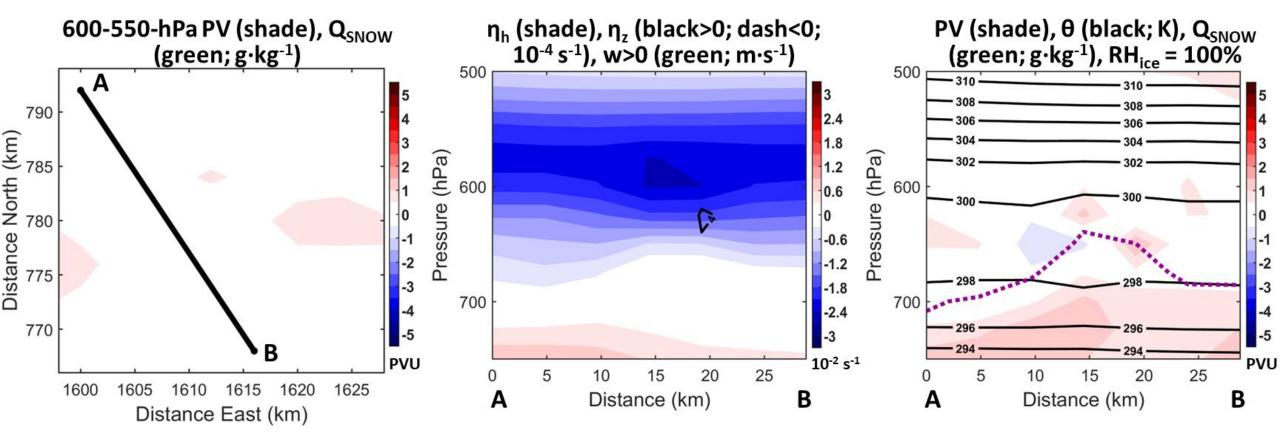
123 h 50 min



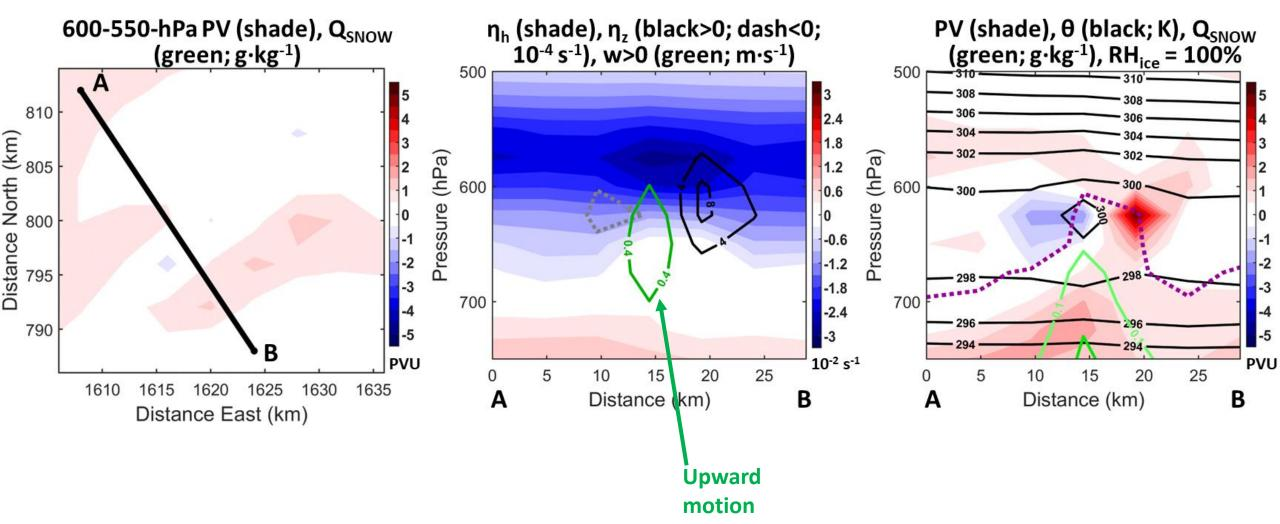
123 h 50 min



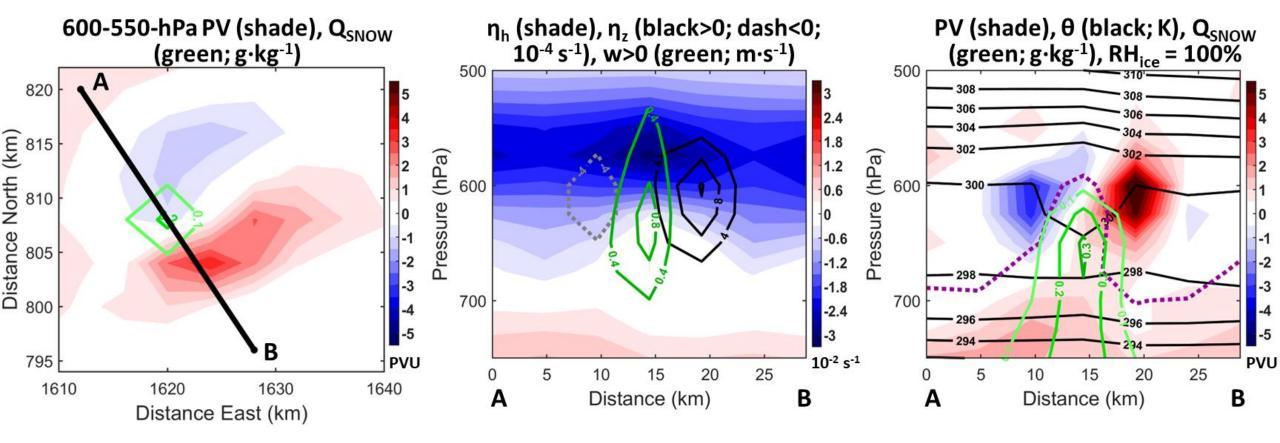
124 h 00 min



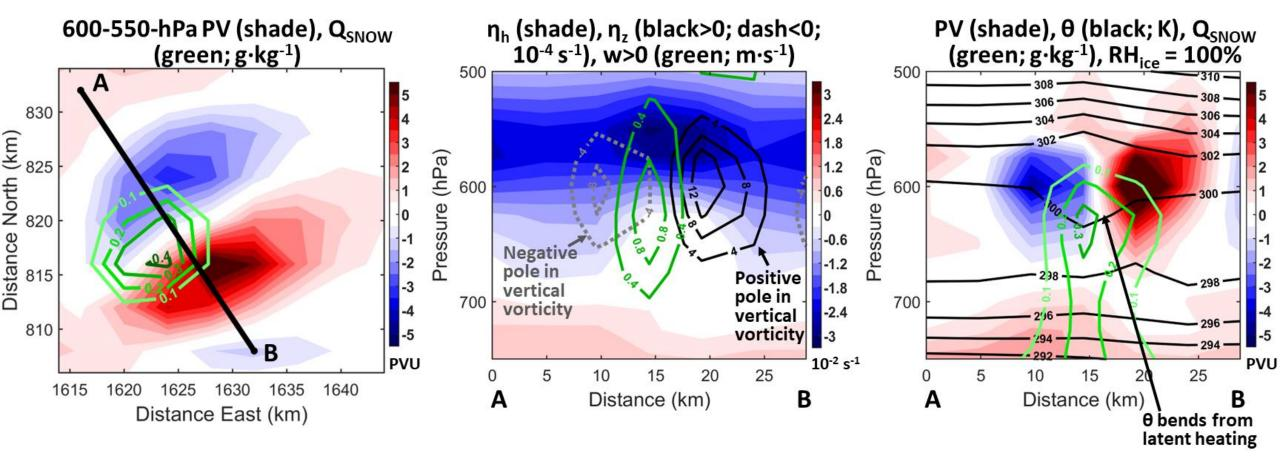
124 h 20 min



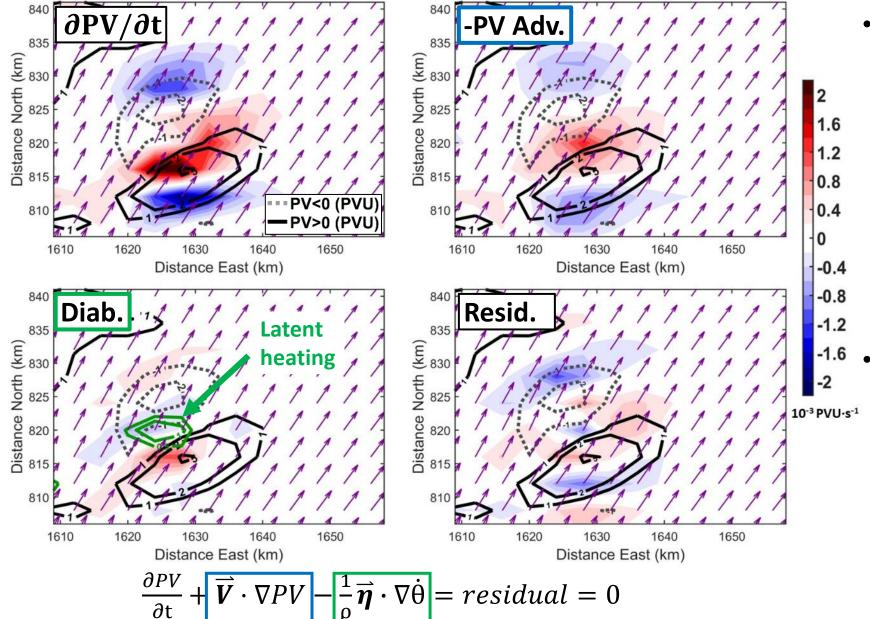
124 h 30 min



124 h 40 min



124 h 40 min: 600-550-hPa PV Tend. Terms (shade), PV (contour), Wind



Diabatic

Advection

- Diagnosed the terms in the 600-550-hPa PV tendency equation as the PV dipole expanded.
 - Time derivatives are approximated with CFD of 2minute output.
 - Diabatic heating rate $(\dot{\theta})$ is approximated by subtracting θ advection from the time-rate-of-change in θ .
- The diabatic term is contributing near the center of the dipole.

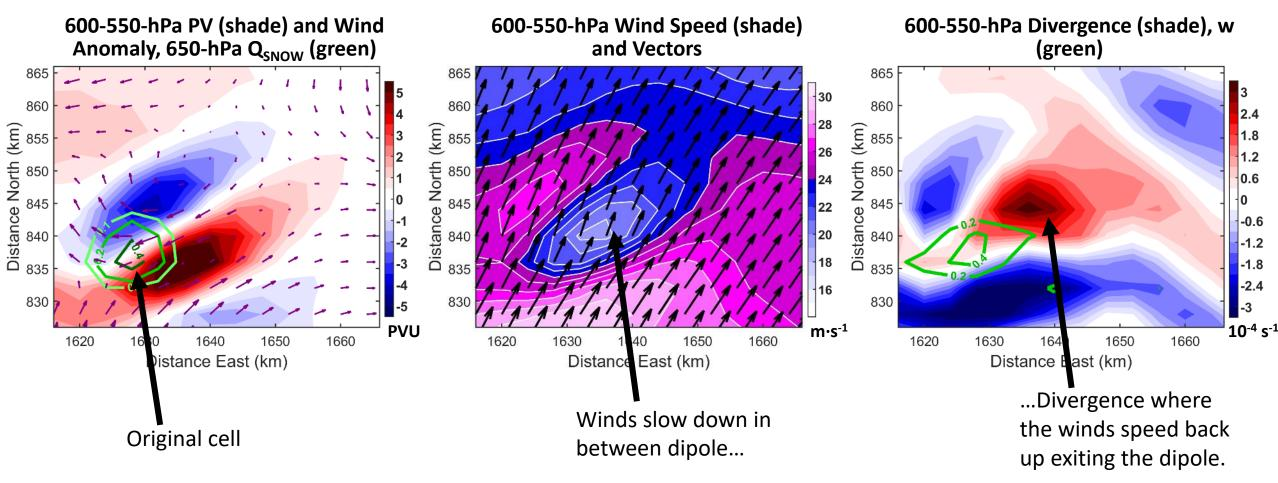
125 h 10 min: 600-550-hPa PV Tend. Terms (shade), PV (contour), Wind -PV Adv. 855 855 Distance North (km)
828
840
828 0.8 PV<0 (PVU) 830 830 0.4 1660 1620 1640 1640 1650 1650 1620 Distance East (km) Distance East (km) -0.4 -0.8 Resid Diab. 855 -1.2 Distance North (km)
828
840
840 Distance North (km)
828
840
878
878
878 -1.6-2 10⁻³ PVU·s⁻¹ 830 1640 1650 1660 1620 1640 1650 1660 1620 Distance East (km) Distance East (km) $|\vec{\eta} \cdot \nabla \dot{\theta}| = residual = 0$

Diabatic

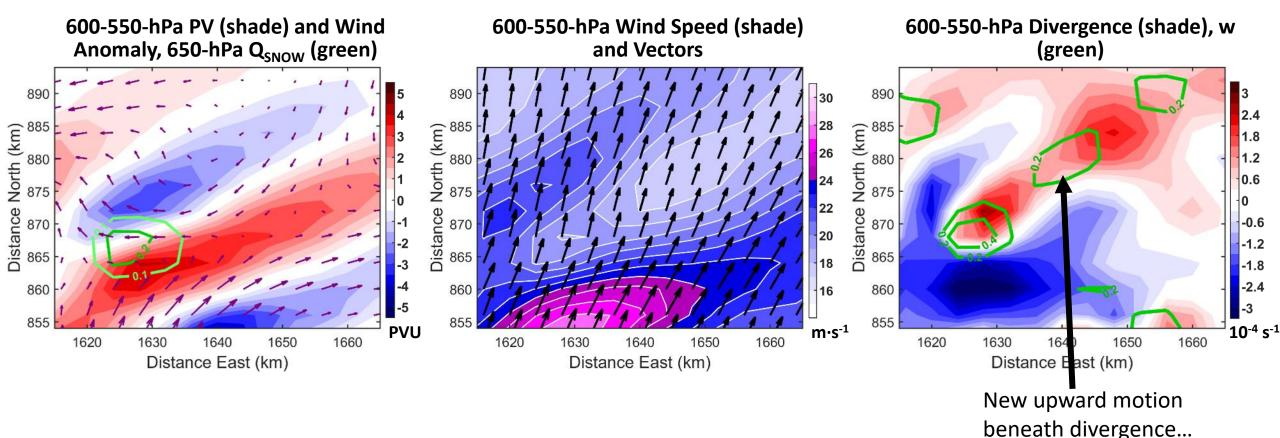
Advection

- Diagnosed the terms in the 600-550-hPa PV tendency equation as the PV dipole expanded.
 - Time derivatives are approximated with CFD of 2minute output.
 - Diabatic heating rate $(\dot{\theta})$ is approximated by subtracting θ advection from the time-rate-of-change in θ .
- The diabatic term is contributing near the center of the dipole.
- Advection corresponds to >90% of NE expansion of PV after it's created from below (at the NE edge of PV dipoles).

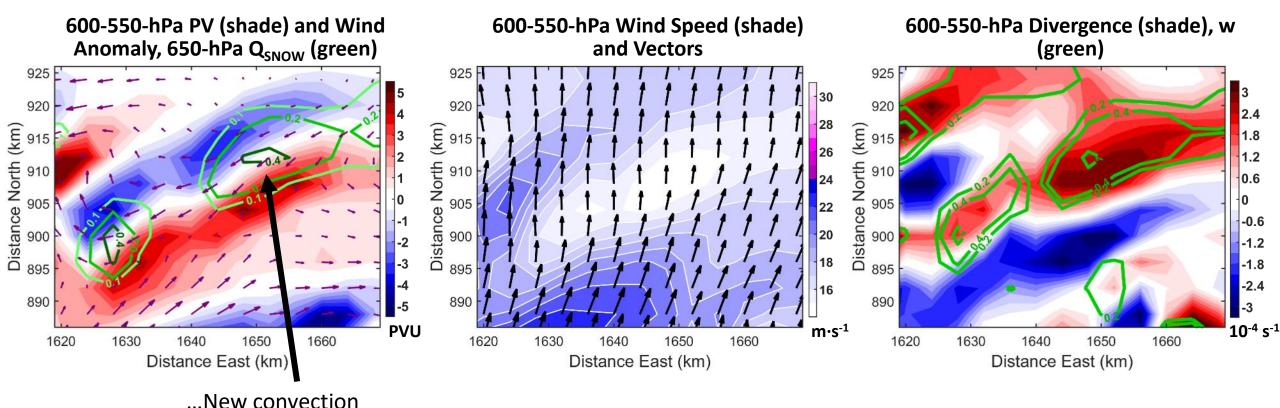
125 h 00 min



125 h 30 min

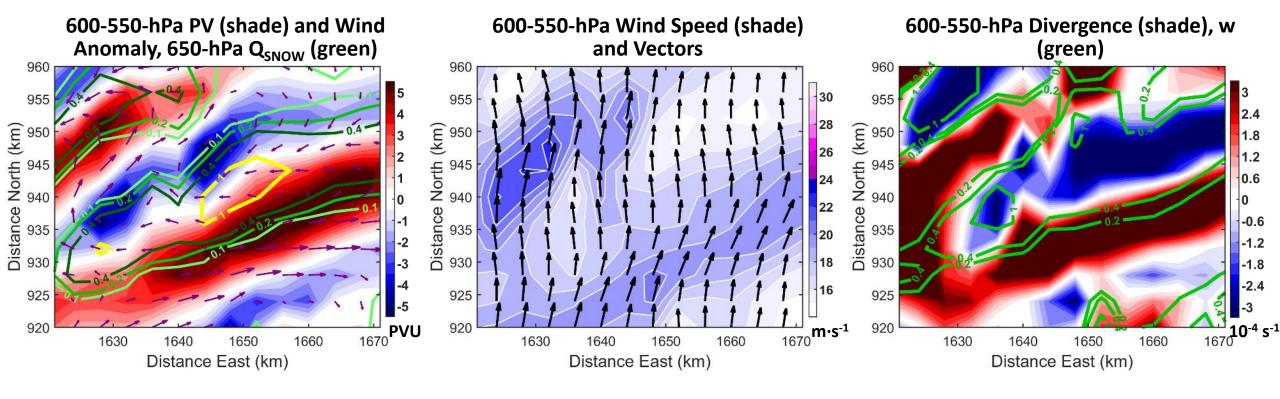


126 h 00 min



beneath divergence

126 h 30 min

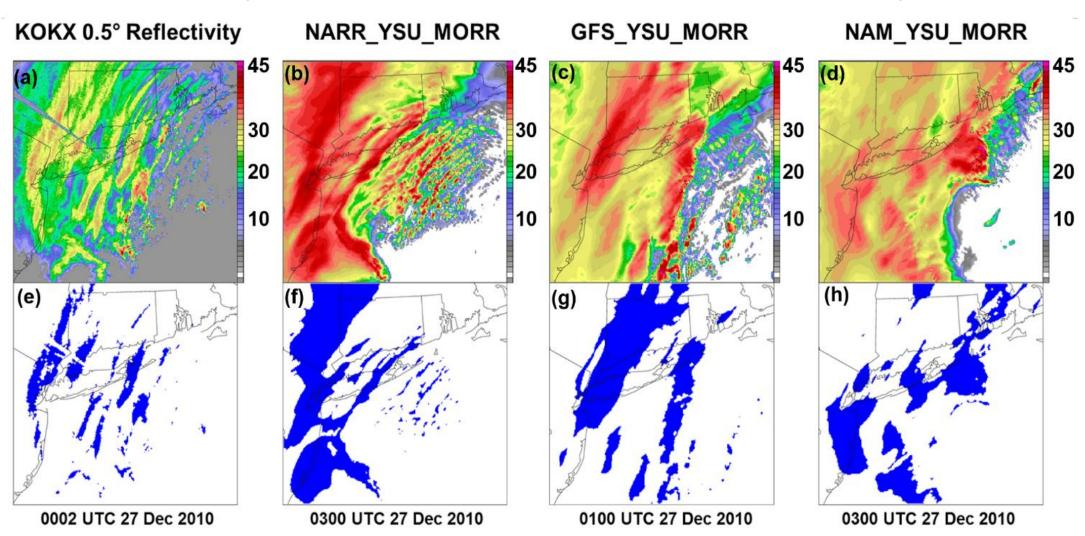


Objectives

- Nested runs of an idealized baroclinic wave model are used to answer the following questions:
 - 1. How do the precipitation structures in the comma head evolve as the cyclone develops?
 - 2. How do changes in the ambient frontogenesis (forcing), vertical shear, and instability around the cyclone relate to changes in the precipitation structures.
 - 3. What mechanisms cause the bands to elongate and persist?
 - 4. How sensitive is the development of the multi-bands to small changes in the initial conditions?

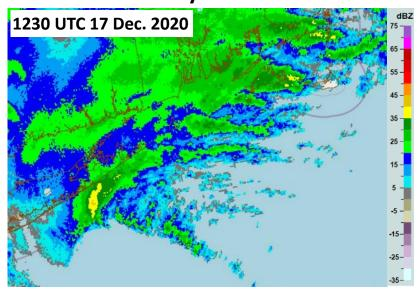
Forecast Challenges

Snowband Predictability Issues (2-km WRF runs of Dec 2010 Event)



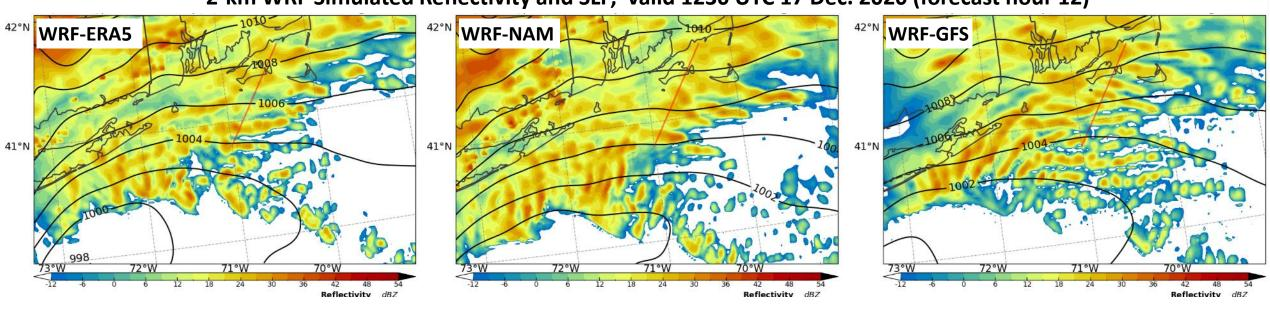
Snowband Predictability Issues (2-km WRF runs of Dec 2020 Event)

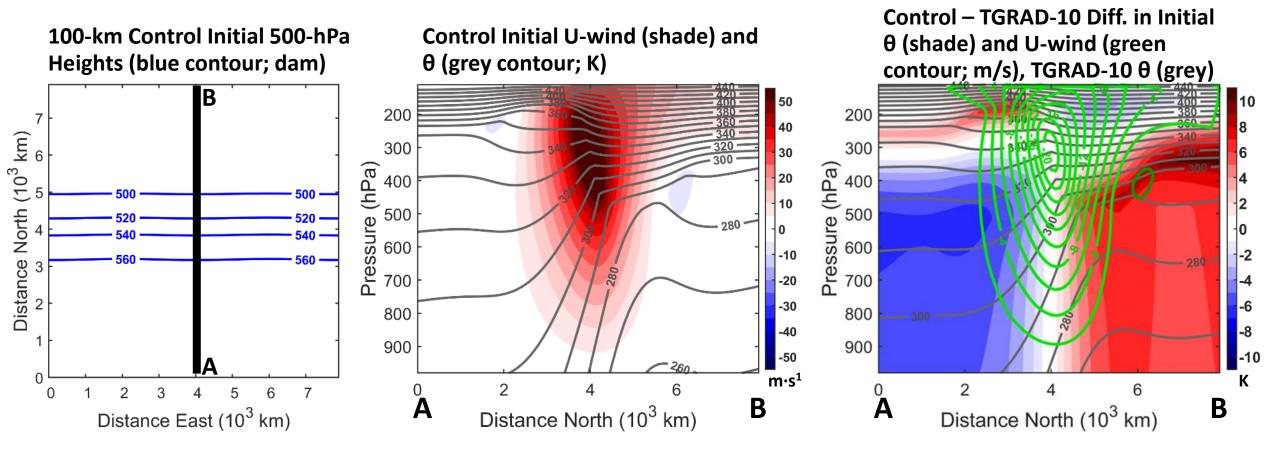
MRMS Reflectivity



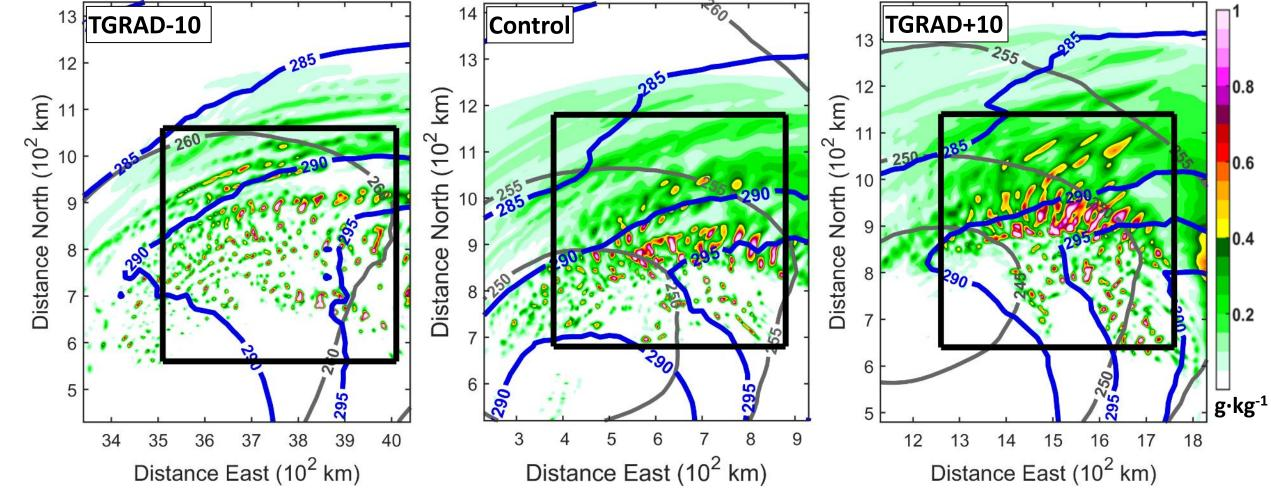
- WRF runs with same PBL and MP schemes, but different initial conditions.
- Each run generally produced multi-bands in this case.
- The extent of the banding and band orientation/morphology were sensitive to the initial conditions.

2-km WRF Simulated Reflectivity and SLP, valid 1230 UTC 17 Dec. 2020 (forecast hour 12)

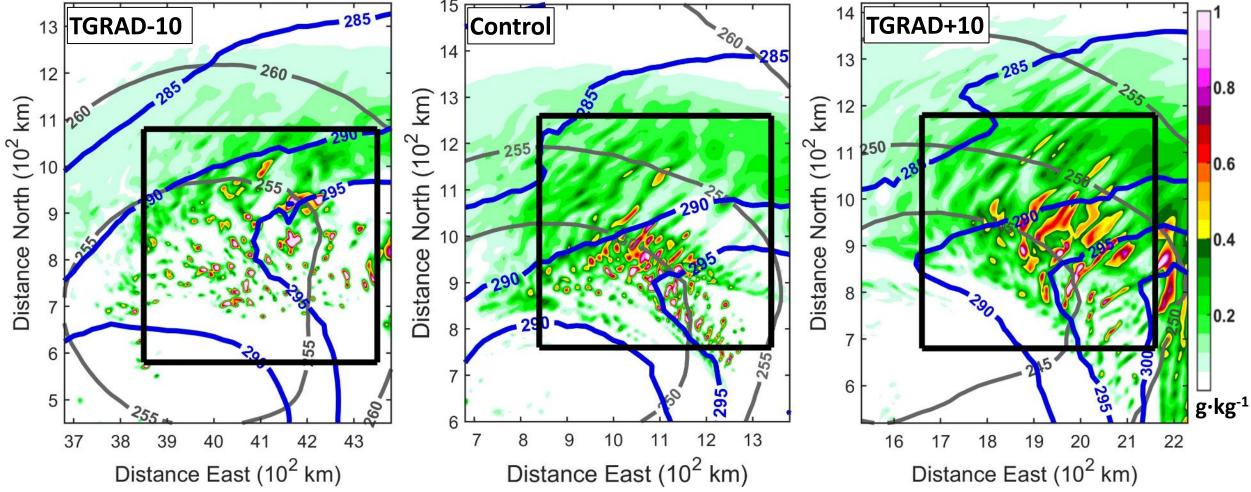




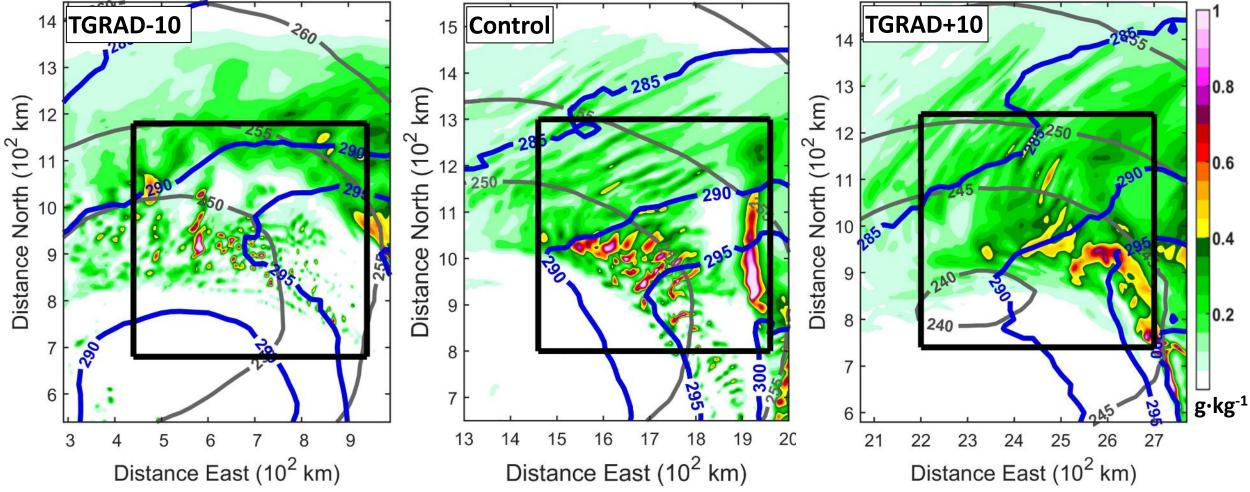
• Perturbed the initial conditions of the control run by decreasing or increasing the horizontal temperature gradient at each vertical level throughout the domain by 10% ("TGRAD-10" and "TGRAD+10", respectively).



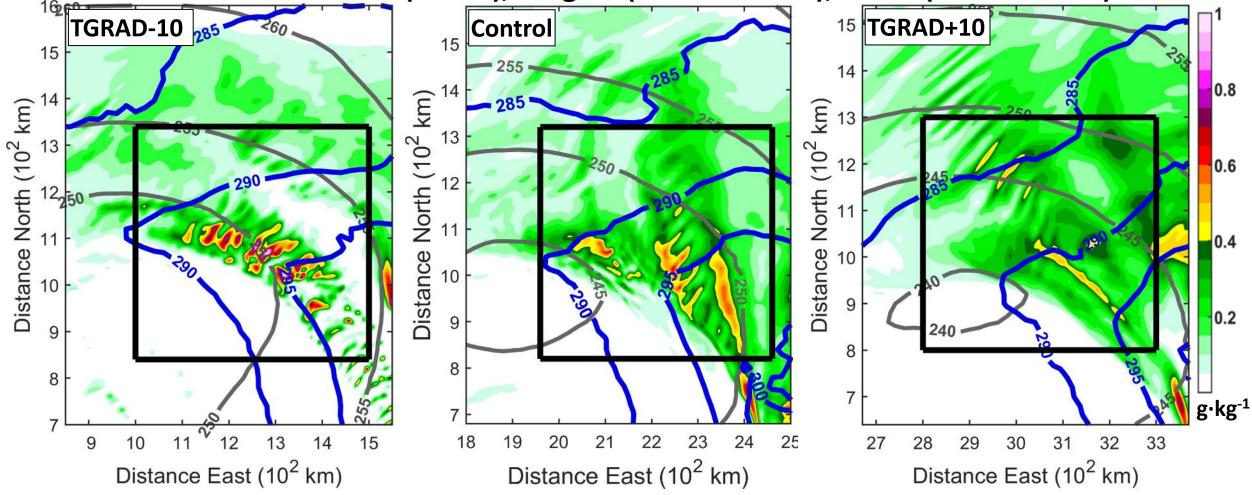
- Decreasing the initial horizontal temperature gradient by 10% delays multi-band until ~138 h.
- Increasing the gradient causes the multi-bands to develop/mature at ~120 h, at least 6 hours earlier than the Control.
 The activity then weakens after ~129 h.



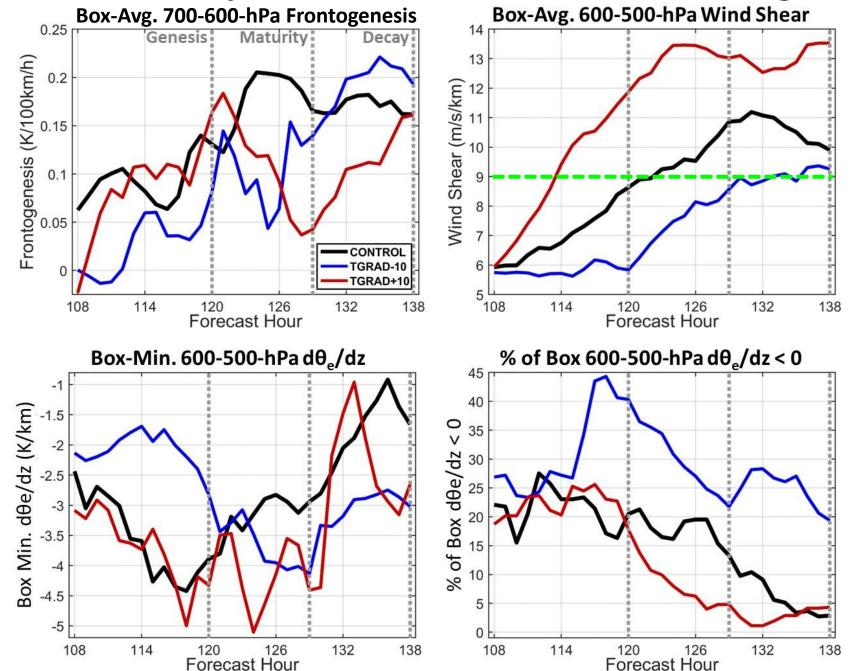
- Decreasing the initial horizontal temperature gradient by 10% delays multi-band until ~138 h.
- Increasing the gradient causes the multi-bands to develop/mature at ~120 h, at least 6 hours earlier than the Control.
 The activity then weakens after ~129 h.



- Decreasing the initial horizontal temperature gradient by 10% delays multi-band until ~138 h.
- Increasing the gradient causes the multi-bands to develop/mature at ~120 h, at least 6 hours earlier than the Control. The activity then weakens after ~129 h.



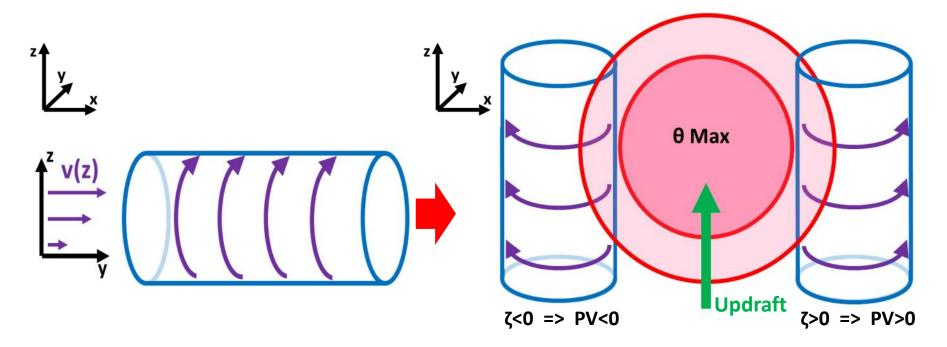
- Decreasing the initial horizontal temperature gradient by 10% delays multi-band until ~138 h.
- Increasing the gradient causes the multi-bands to develop/mature at ~120 h, at least 6 hours earlier than the Control.
 The activity then weakens after ~129 h.



- TGRAD-10 and TGRAD+10 shear >9 m/s/km at ~136 h and 114 h, respectively.
- TGRAD-10 PI grows ~9 hours later, reaching -4 K/km by ~129 h.

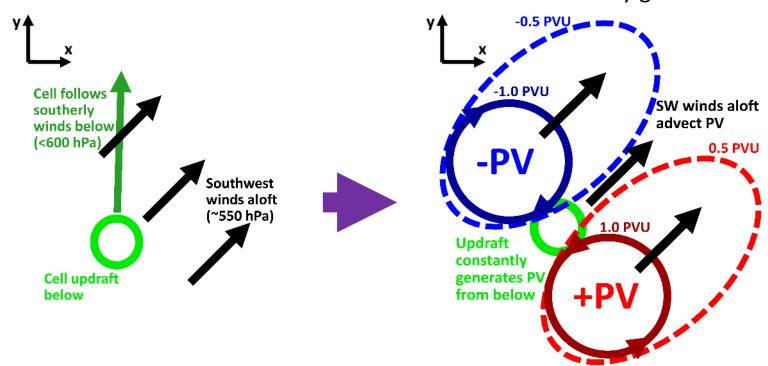
Summary of Conceptual Model

- The 4-km baroclinic wave model develops multi-bands east of the surface low at 120-138 h. The bands start as cells that elongate and deepen as they move northward around the low.
- The activity coincides with a growth in 700-500-hPa PI east of the low and an increase in 600-500-hPa vertical shear. The activity dissipates after the instability is depleted.
- Bands expand northeastward due to a feedback between PV dipoles and ambient flow.
 - A cell updraft below 600-hPa tilts the 600-550-hPa horizontal absolute vorticity into the vertical. Latent heating in the updraft changes the local θ gradient, resulting in a PV dipole at 600-550-hPa.



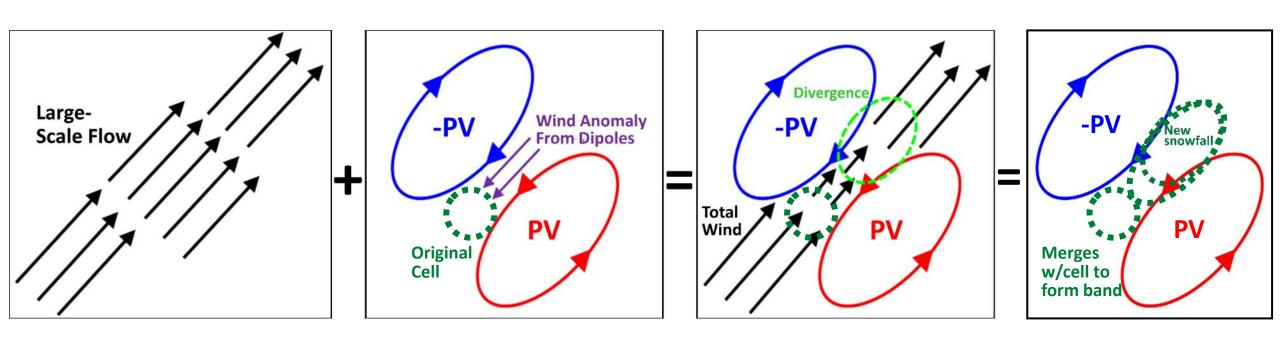
Summary of Conceptual Model

- The 4-km baroclinic wave model develops multi-bands east of the surface low at 120-138 h. The bands start as cells that elongate and deepen as they move northward around the low.
- The activity coincides with a growth in 700-500-hPa PI east of the low and an increase in 600-500-hPa vertical shear. The activity dissipates after the instability is depleted.
- Bands expand northeastward due to a feedback between PV dipoles and ambient flow.
 - A cell updraft below 600-hPa tilts the 600-550-hPa horizontal absolute vorticity into the vertical. Latent heating in the updraft changes the local θ gradient, resulting in a PV dipole at 600-550-hPa.
 - Southwest winds ~550-hPa advect the PV northeastward as it is continuously generated from below.



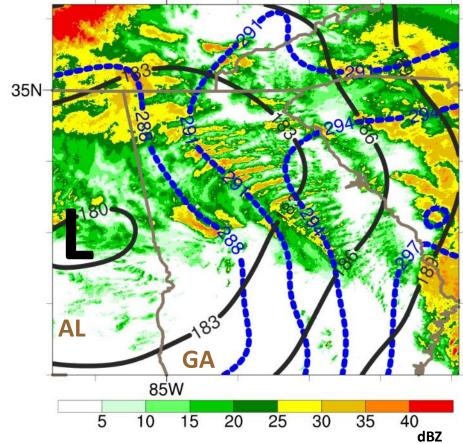
Summary of Conceptual Model (continued)

- The dipoles affect where the new convection develops- a line NE from the original cell.
- The circulations from the 2 PV poles cause a NE flow anomaly in between them, opposing the large-scale 600-550-hPa SW flow. Thus, the total wind slows down entering the dipole and speeds up exiting it. The latter corresponds to divergence (closer to 550-hPa) extending NE from the dipole. New upward motion and snow develop from beneath this divergence.
- The band dissipates over ~2-3 h after it moves away from the PI and shear. Gradual PV destruction from evaporative cooling north and south of the band.

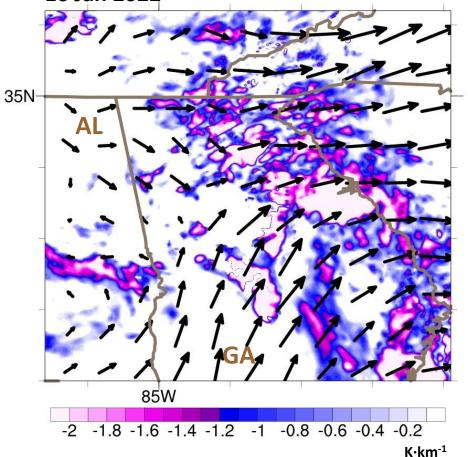


Conclusions and Takeaways for Forecasters

MRMS Reflectivity (shade), HRRR ANL 700-hPa height (black contour) and θ (blue), valid 1500 UTC 16 Jan 2022



HRRR ANL 750-550-hPa $d\theta_e/dz$ (shade) and Wind Shear Vectors, valid 1500 UTC 16 Jan 2022



- PI east of the surface low is the dominant instability in the development of multiband convection.
- Mid-level vertical shear is crucial in the organization/growth of the multi-bands.
- The development of both parameters in forecasts can be highly sensitive to the initial conditions.

References

- Chagnon, J. M., and S. L. Gray, 2009: Horizontal Potential Vorticity Dipoles on the Convective Storm Scale. Q. J. R. Meteorol. Soc., 135, 1392–1408. https://doi.org/10.1002/qj.468.
- Ganetis, S. A., B. A. Colle, S. E. Yuter, and N. P. Hoban, 2018: Environmental Conditions Associated with Observed Snowband Structures Within Northeast U.S. Winter Storms. *Mon. Wea. Rev.*, **146**, 3675—3690. DOI:10.1175/MWR-D-18-0054.1.
- Hitchman, M. H., and S. M. Rowe, 2019: On the Structure and Formation of UTLS PV Dipole/Jetlets in Tropical Cyclones by Convective Momentum Surges. *Mon. Wea. Rev.*, **147**, 4107-4125, doi: 10.1175/MWR-D-18-0232.1
- Keeler, K. M., B. F. Jewett, R. M. Rauber, G. M. McFarquhar, R. M. Rasmussen, L. Xue, C. Liu, and G. Thompson, 2016: Dynamics of Cloud-Top Generating Cells in Winter Cyclones. Part I: Idealized Simulations in the Context of Field Observations. *J. Atmos. Sci.*, **73**, 1507-1527. DOI:10.1175/JAS-D-15-0126.1.
- Leonardo, N., and B. Colle, 2024 (in press): Analysis of Snow Multi-Bands and Their Environments with High-Resolution Idealized Simulations. *Mon. Wea. Rev.*, doi: 10.1175/MWR-D-23-0211.1
- Moon, Y. and D. S. Nolan, 2015: Spiral Rainbands in a Numerical Simulation of Hurricane Bill (2009).
 Part I: Structures and Comparisons to Observations. *J. Atmos. Sci.*, 72, 164-190, doi: https://doi.org/10.1175/JAS-D-14-0058.1

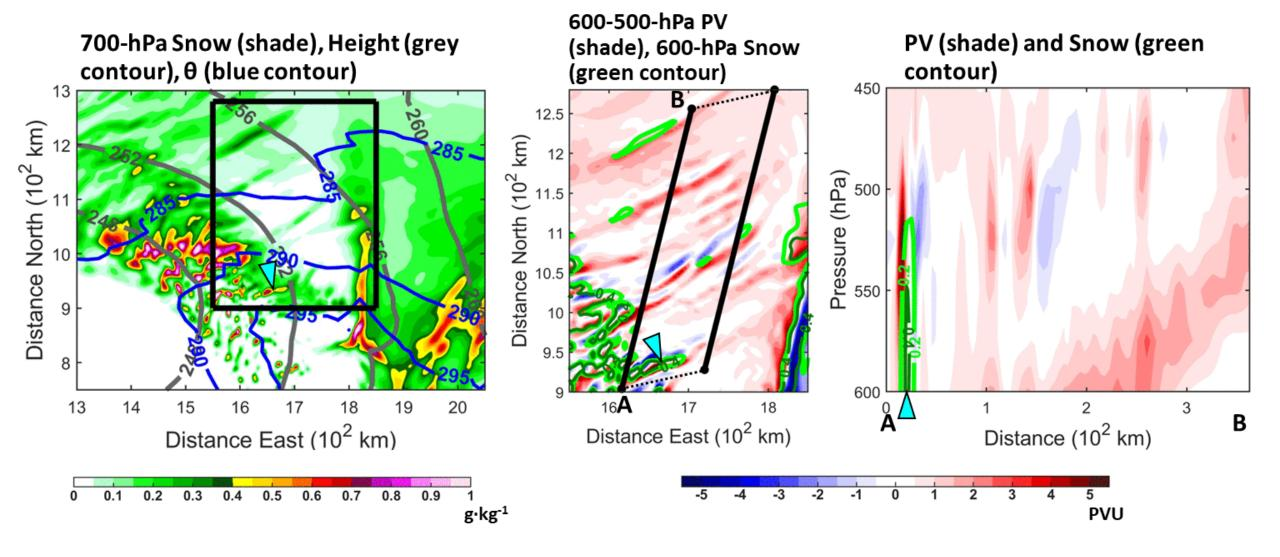
References

- Norris, J., G. Vaughan, and D. M. Schultz, 2014: Precipitation Banding in Idealized Baroclinic Waves. *Mon. Wea. Rev.*, **142**, 3081–3099, doi: 10.1175/MWR-D-13-00343.1
- Norris, J., G. Vaughan, and D. M. Schultz, 2017: Variability of Precipitation Along Cold Fronts in Idealized Baroclinic Waves. *Mon. Wea. Rev.*, **145**, 2971–2992, doi: 10.1175/MWR-D-16-0409.1
- Novak, D. R., J. S. Waldstreicher, D. Keyser, and L. F. Bosart, 2006: A Forecast Strategy for Anticipating Cold Season Mesoscale Band Formation within Eastern U.S. Cyclones. *Wea. Forecasting*, **21**, 3–23, https://doi.org/10.1175/WAF907.1.
- Rosenow, A. A., D. M. Plummer, R. M. Rauber, G. M. McFarquhar, B. F. Jewett, and D. Leon, 2014:
 Vertical Velocity and Physical Structure of Generating Cells and Convection in the Comma Head Region of Continental Winter Cyclones. *J. Atmos. Sci.*, 71, 1538–1558. DOI:10.1175/JAS-D-13-0249.1
- Sanders, F., and L. F. Bosart, 1985: Mesoscale structure in the Megalopolitan Snowstorm of 11–12 February 1983. Part I: Frontogenetical Forcing and Symmetric Instability. *J. Atmos. Sci.*, **42**, 1050–1061, https://doi.org/10.1175/1520-0469(1985)042,1050:MSITMS.2.0.CO;2.
- Skamarock, W., J. B. Klemp, J. Dudhia, D. O. Gill, D. Barker, M. G. Duda, X. -Y. Huang, and W. Wang, 2008: A Description of the Advanced Research WRF Version 3. NCAR Technical Note NCAR/TN-475+STR. DOI:10.5065/D68S4MVH.
- Xu, Q., 1992: Formation and Evolution of Frontal Rainbands and Geostrophic Potential Vorticity Anomalies. J. Atmos. Sci., 49, 629–648, DOI:10.1175/1520-0469(1992)049,0629:FAEOFR.2.0.CO;2.

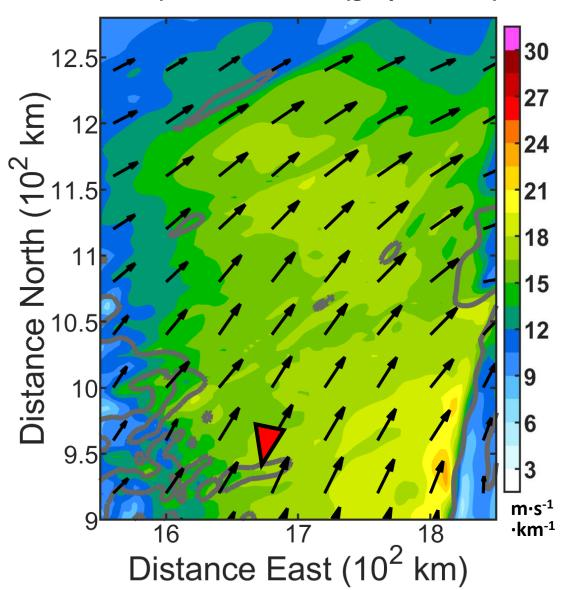
Thank you!

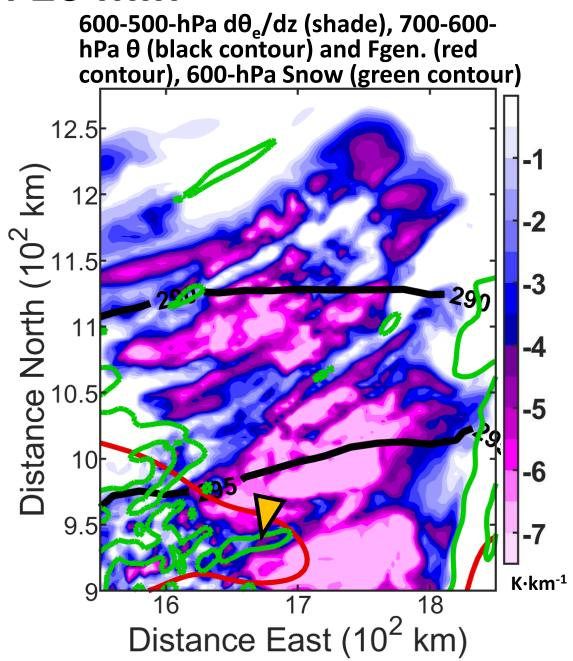
Extra Slides

126 h 20 min

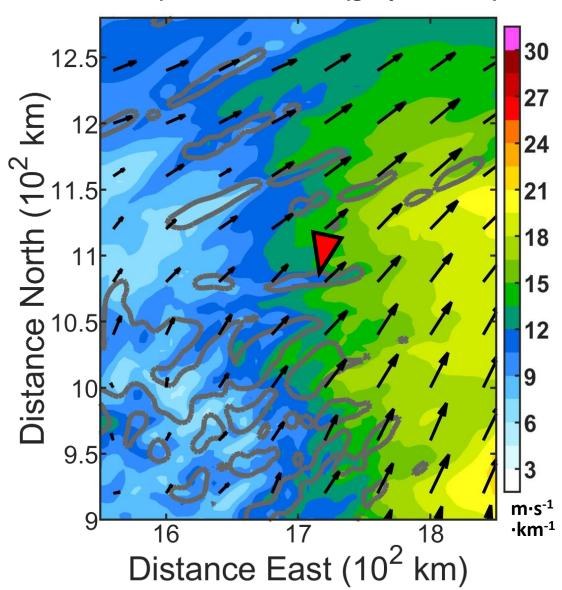


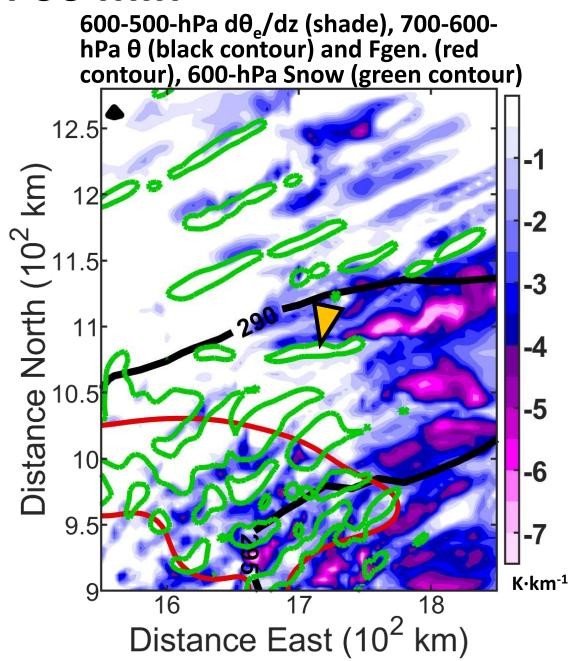
126 h 20 min



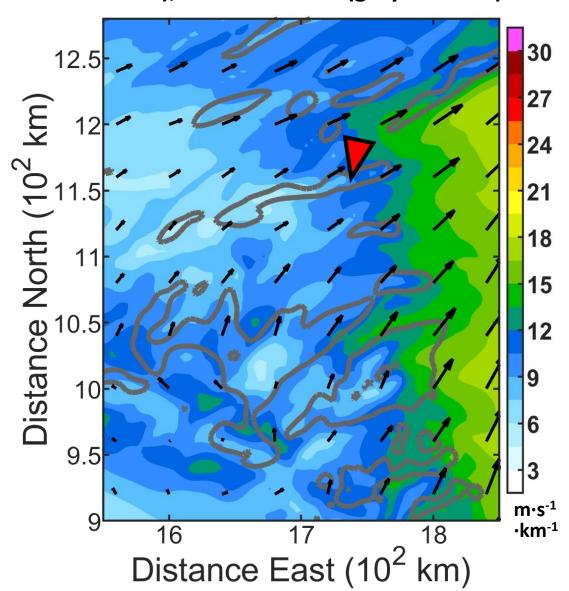


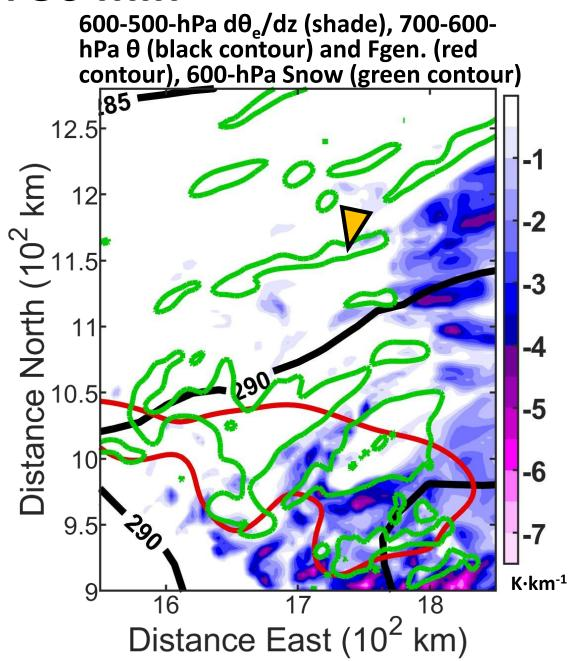
128 h 00 min



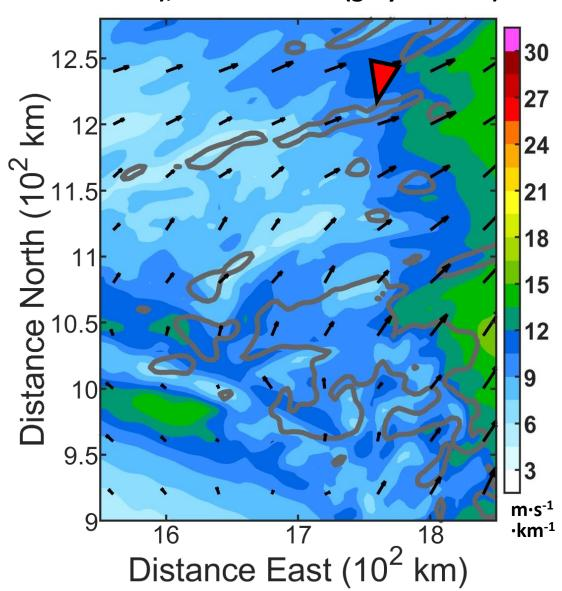


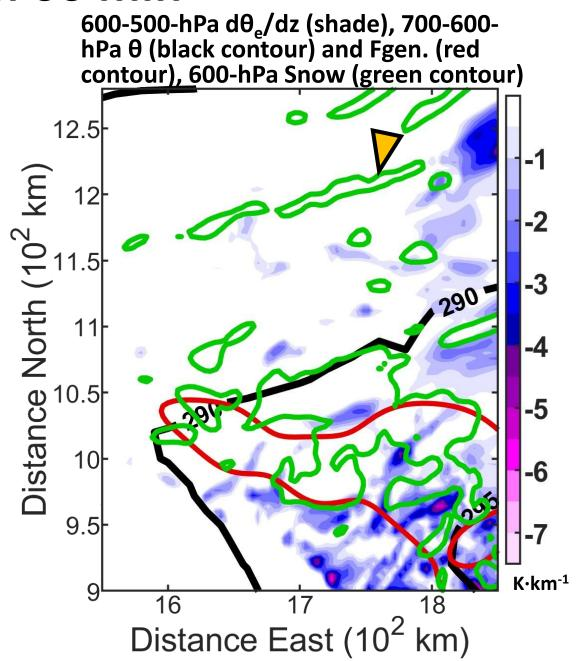
129 h 30 min



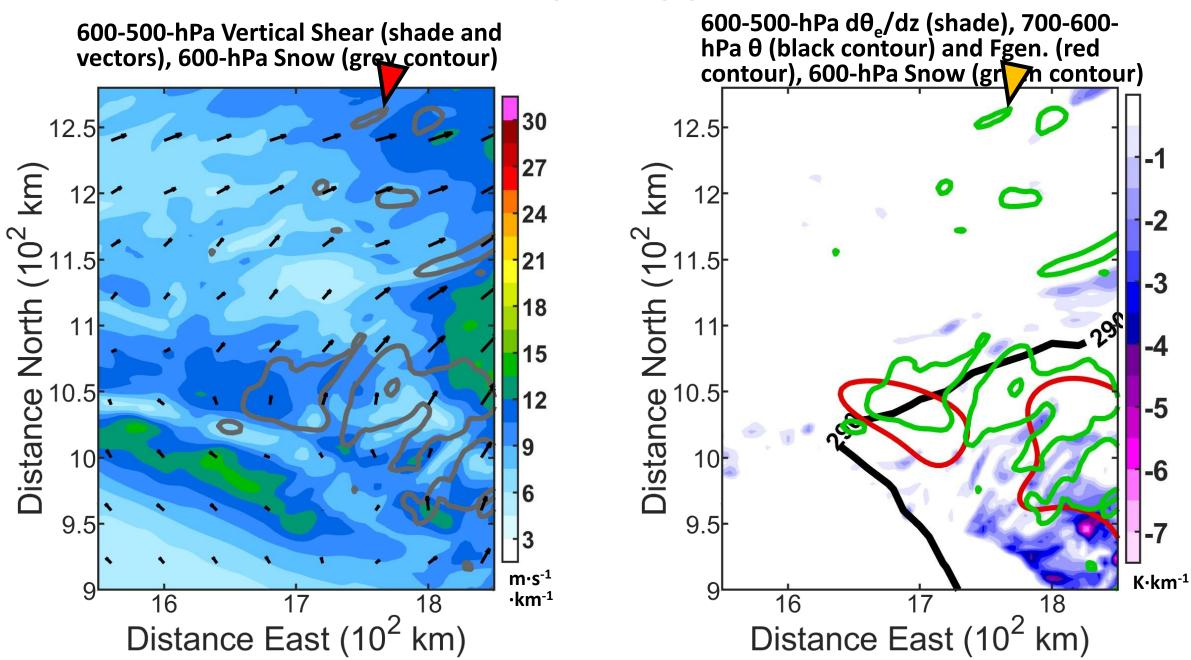


131 h 00 min





131 h 00 min



• PV equation:
$$PV = \frac{1}{\rho} \overrightarrow{\boldsymbol{\omega}_{a}} \cdot \nabla \theta = \frac{1}{\rho} \left(\left(\frac{\partial w}{\partial y} - \frac{\partial v}{\partial z} \right) \frac{\partial \theta}{\partial x} + \left(\frac{\partial u}{\partial z} - \frac{\partial w}{\partial x} \right) \frac{\partial \theta}{\partial y} + \left(\frac{\partial v}{\partial x} - \frac{\partial u}{\partial y} + f \right) \frac{\partial \theta}{\partial z} \right)$$

- <u>PV tendency</u>: $\frac{\partial PV}{\partial t} + \overrightarrow{V} \cdot \nabla PV \frac{1}{\rho} \overrightarrow{\omega_a} \cdot \nabla \dot{\theta} = resid.$
- <u>Diabatic Term</u>: $\frac{1}{\rho} \overrightarrow{\boldsymbol{\omega_a}} \cdot \nabla \dot{\boldsymbol{\theta}} = \frac{1}{\rho} \left(\left(\frac{\partial w}{\partial y} \frac{\partial v}{\partial z} \right) \frac{\partial \dot{\boldsymbol{\theta}}}{\partial x} + \left(\frac{\partial u}{\partial z} \frac{\partial w}{\partial x} \right) \frac{\partial \dot{\boldsymbol{\theta}}}{\partial y} + \left(\frac{\partial v}{\partial x} \frac{\partial u}{\partial y} + f \right) \frac{\partial \dot{\boldsymbol{\theta}}}{\partial z} \right)$

where \overrightarrow{V} is the 3D wind, $\overrightarrow{\omega_a}$ is the 3D absolute vorticity, and $\dot{\theta}$ is the diabatic heating rate.

- Derivatives are approximated with CFD, using 2-minute output.
- Next 4 slides:
 - <u>Left</u>: 600-500-hPa $\partial PV/\partial t$ (shade) and PV (black contour > 0 PVU, grey dash < 0 PVU), and 600-hPa snow mixing ratio (green contour; g·kg⁻¹).
 - Middle: 600-500-hPa PV advection (shade), PV, and wind vectors.
 - Right: 600-500-hPa diabatic term (shade), PV, and diabatic heating rate (dark green contour>0, light green dash<0; 10^{-3} K·s⁻¹).

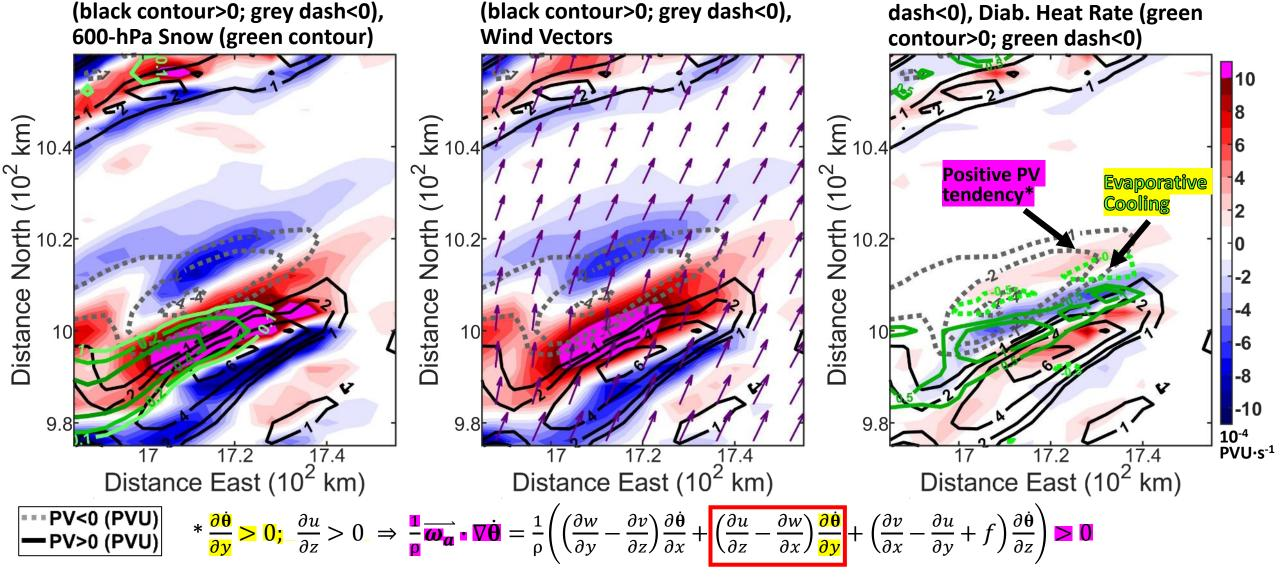
127 h 00 min

600-500-hPa PV Adv. (shade), PV

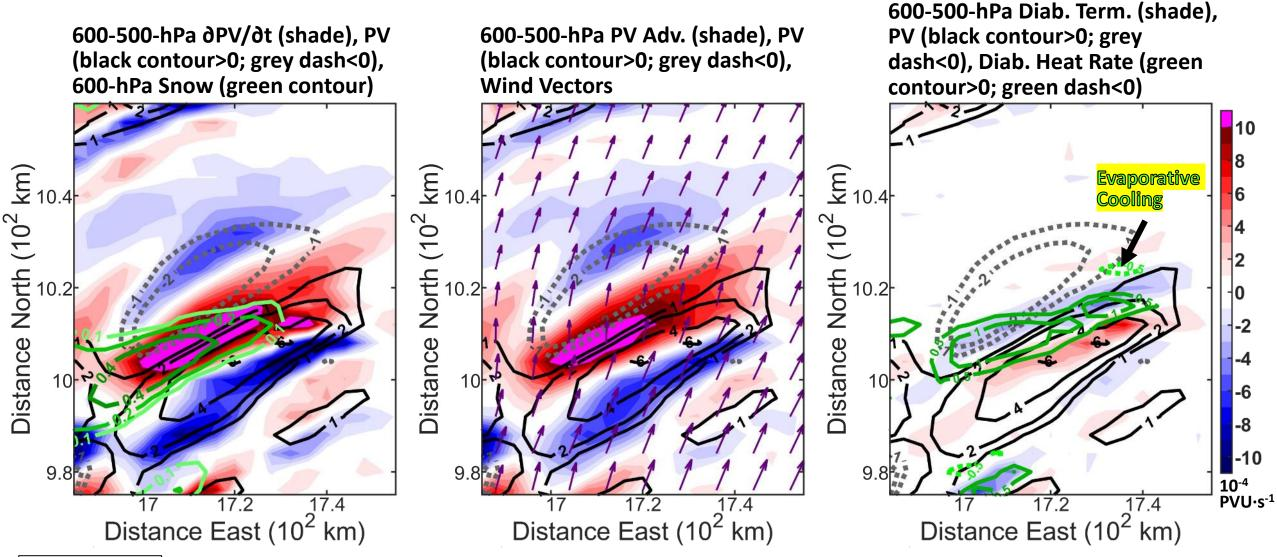
600-500-hPa ∂PV/∂t (shade), PV

600-500-hPa Diab. Term. (shade),

PV (black contour>0; grey



127 h 10 min

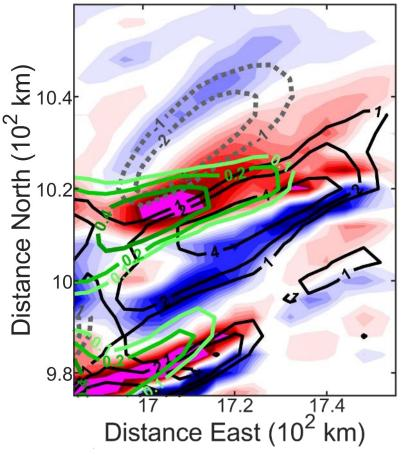


PV<0 (PVU)
PV>0 (PVU)

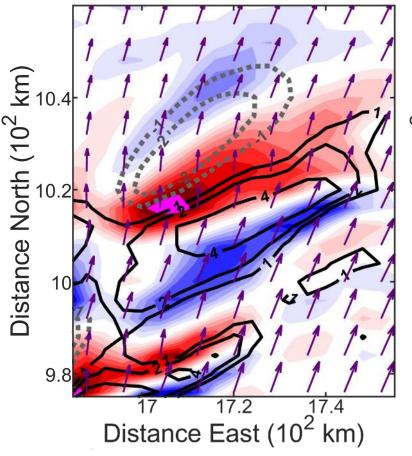
 While the diabatic cooling weakens, it has a cumulative impact on the temperature field, increasing the cold anomaly and thus the northward temperature gradient (and PV).

127 h 20 min

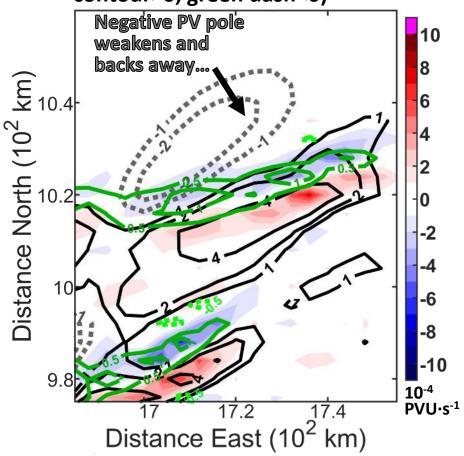
600-500-hPa dPV/dt (shade), PV (black contour>0; grey dash<0), 600-hPa Snow (green contour)

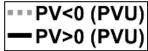


600-500-hPa PV Adv. (shade), PV (black contour>0; grey dash<0), Wind Vectors

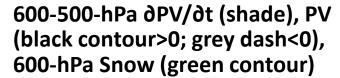


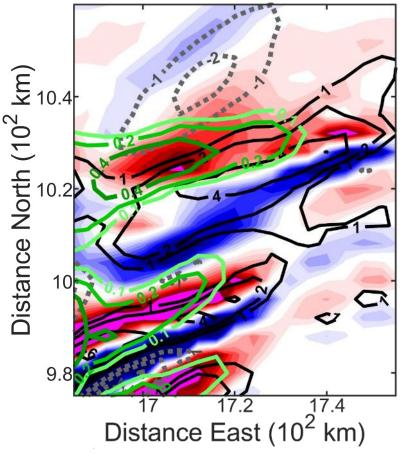
600-500-hPa Diab. Term. (shade), PV (black contour>0; grey dash<0), Diab. Heat Rate (green contour>0; green dash<0)



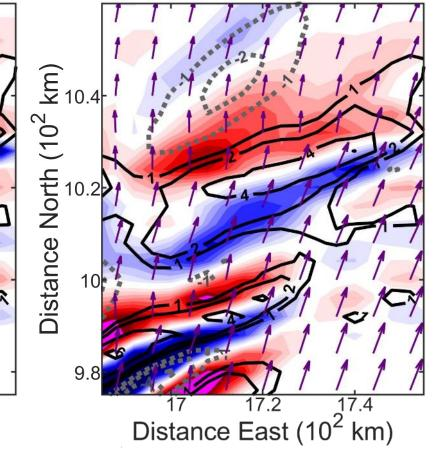


127 h 30 min

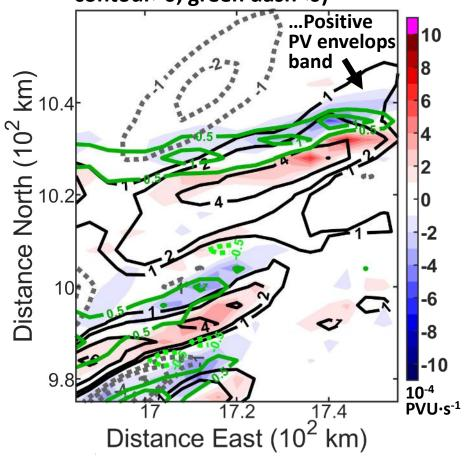


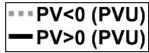


600-500-hPa PV Adv. (shade), PV (black contour>0; grey dash<0), Wind Vectors

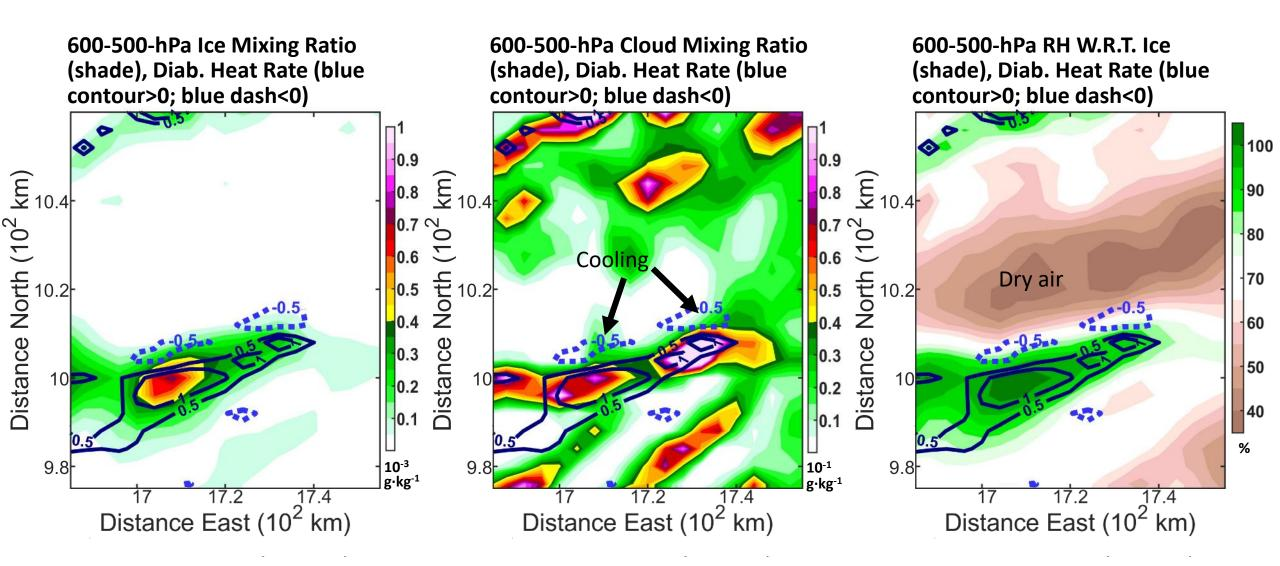


600-500-hPa Diab. Term. (shade), PV (black contour>0; grey dash<0), Diab. Heat Rate (green contour>0; green dash<0)



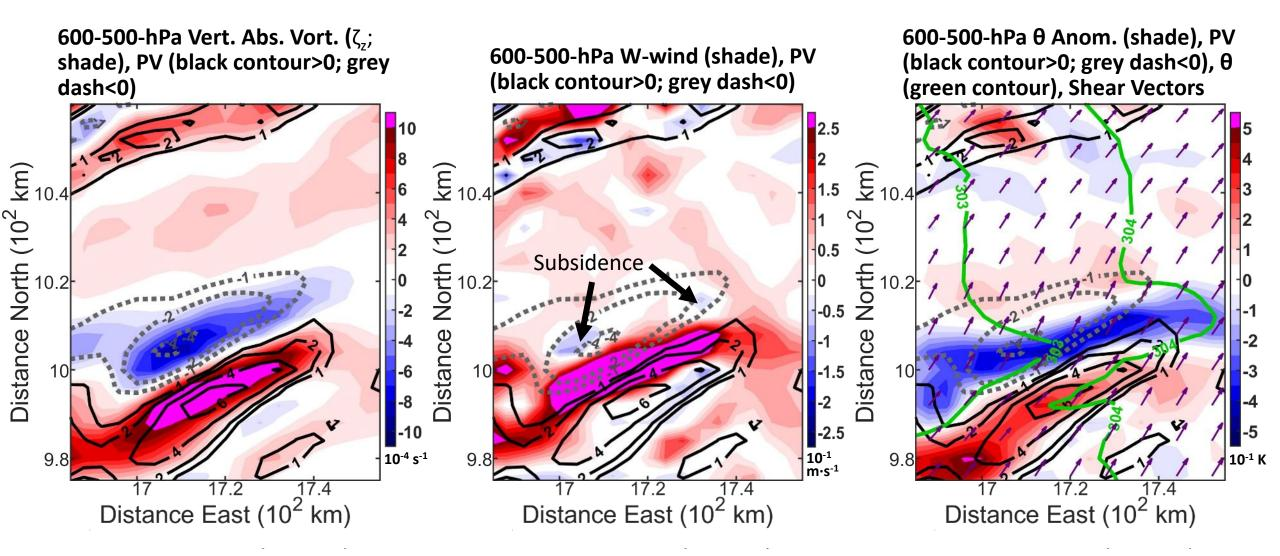


127 h 00 min



 Region of cooling on outer fringes of band, within QCLOUD and QICE extending into the subsaturated air.

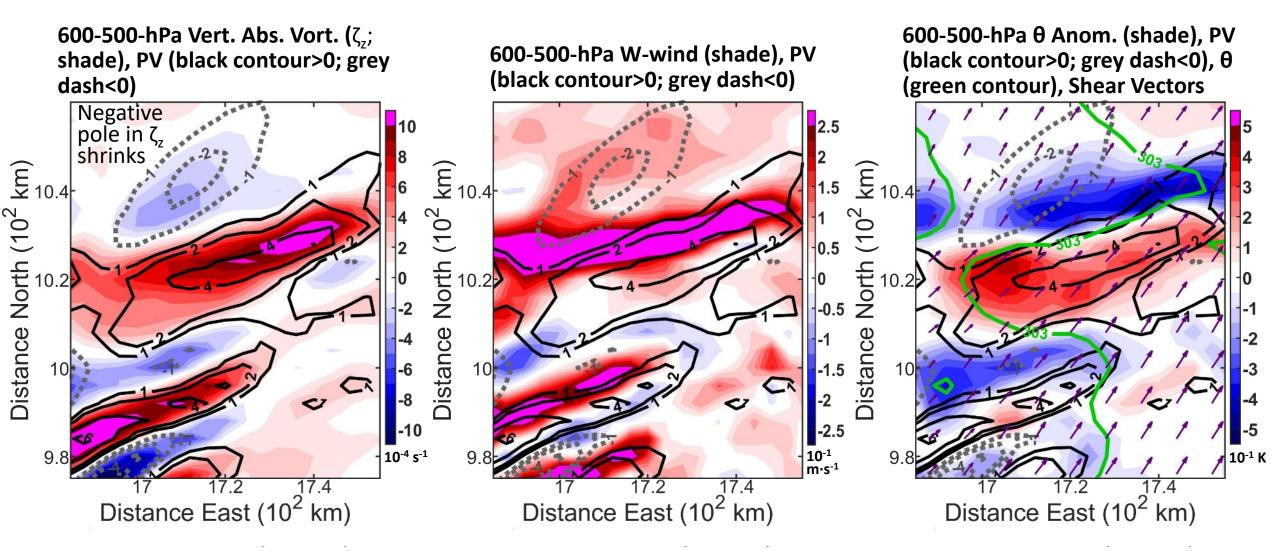
127 h 00 min



PV<0 (PVU)
PV>0 (PVU)

Subsidence within cold air anomaly.

127 h 30 min



---PV<0 (PVU) ---PV>0 (PVU)

 Cold subsidence redistributes horizontal absolute vorticity into the vertical in a dipole opposite of the one created by latent heating and ascent-> cancels-out the negative absolute vorticity.